Equatorial Energy Accumulation and Emanation Regions: Impacts of a Zonally Varying Basic State

PETER J. WEBSTER AND HAI-RU CHANG

The Pennsylvania State University, Department of Meteorology, University Park, Pennsylvania

(Manuscript received 8 October 1986, in final form 11 September 1987)

ABSTRACT

Previous studies have suggested that the regions of mean anomalous perturbation kinetic energy which exist in the vicinity of the equatorial upper-tropospheric westerlies are the result of the propagation of *extratropical* synoptic and low frequency waves through the equatorial "westerly duct" where a subsequent wave energy convergence occurs. The proposition that these perturbed equatorial regions may arise from remote equatorial energy sources is investigated. It is shown that three criteria must be met. The first two, the existence of wave energy sources along the equator and a mechanism to transport that energy longitudinally, are accounted for relatively easily with existing theory of divergent, trapped equatorial modes. The third criterion, the requirement of a mechanism for an accumulation of transient energy in the equatorial stretch flow (i.e., nonzero $\bar{u}_x$), is not immediately obvious and requires exploration to develop new concepts.

Using simple WKBJ arguments it is shown that within a realistic parameter range, a combination of longitudinal stretch in the basic state along the equator and the characteristics of the equatorial trapped waves satisfy the third criterion. The equatorial waves must possess a divergent structure which insists on equatorial trapping. It is shown that purely barotropic modes, which cannot be equatorially trapped, do not represent the real atmospheric structure at low latitudes. Regions of negative longitudinal stretch along the equator (i.e., westerlies decreasing, or easterlies increasing, towards the east) are shown to be *wave energy accumulation* regions. Regions with positive stretch, on the other hand, are *wave energy depletion* regions. A free-surface barotropic model with fully nonlinear basic states, containing both stretch and shear, confirm the results of the simpler model, i.e., regardless of the position of the energy source within the tropical atmosphere the wave energy accumulates in the same region; namely, on the eastern side of the westerly maximum. Thus, the third criterion is accounted for by the longitudinal trapping of the equatorial Rossby waves in specific regions as they move through the longitudinal stretch flow. It is argued that the existence of energy depletion and accumulation regions provides for the existence of an *equatorial teleconnection system* allowing for remote regions of the tropics to be connected by the equatorial transient modes. A number of alternate hypotheses such as the instability of the longitudinal varying basic flow are tested, although, in this case, the basic state is found to be very stable, indicating a robustness of the wave energy accumulation hypothesis.

The numerical results indicate that the equatorial wave accumulation regions are also *emanation* regions of equatorial transient influence to higher latitudes. That is, wherever the equatorial regions are excited, a wave train to higher latitudes will originate from the *same* longitude belt along the equator, producing a phase locked response at higher latitudes given the same mean basic equatorial flow. It is argued that the concept of tropical emanation regions provides a significant modification to the tropical-extratropical wave train teleconnection theory.

It is shown that these new theories of atmospheric teleconnections (i.e., the equatorial *and* the modified tropical–extratropical theories) may allow interpretation of some rather difficult questions that have been posed in both modeling and observational studies.

1. Introduction

In the late 1960s a series of observational and theoretical studies provided a new basis for the understanding of the elementary physics of the large-scale tropical atmospheric circulation and were thus revolutionary.

a. Identification of fundamental modes in the tropical atmosphere

Foremost in these studies was Matsuno (1966), which provided new and enlightening perspectives of the tropical atmosphere. It showed that there existed classes of very large-scale modes possessing a mix of divergent and rotational characteristics that were trapped about the equator. Using a simple primitive free-surface barotropic model on an equatorial β-plane, Matsuno described the fundamental structures of these

Corresponding author address: Dr. Peter J. Webster, Department of Meteorology, The Pennsylvania State University, 503 Walker Building, University Park, PA 16802.

newly identified waves: the westward propagating Rossby wave, an eastward and a westward propagating set of gravity waves and two hybrid families; the eastward propagating Kelvin wave and the westward propagating mixed Rossby-gravity wave. The latter is an antisymmetric mode which shows rotational aspects at very large scales but an increasing divergent gravity wave character at smaller scales. Later, the Matsuno solutions were shown to be subsets of general spherical modes by Longuet-Higgins (1968). Implicit in these studies is that the equatorial trapping of the modes is a direct result of their divergent nature. Purely barotropic modes, on the other hand, are not trapped about the equator (see discussion in section 3).

Both Matsuno and Longuet-Higgins considered the fundamental solutions of a quiescent basic state. By simple extension (e.g., Webster, 1972) the structure of equatorial modes in a basic state in solid rotation can be considered. However, the fundamental structure of the modes did not change from those considered by either Matsuno or Longuet-Higgins as the simple basic flow provided only a simple Galilean translation. However, the consideration of the waves in a nonzero, although still zonally *asymmetric,* basic state proved to be important to climate dynamics. It was shown that with realistic basic states, steady-state solutions were possible with planetary stable equatorially trapped modes (Webster, 1972, 1973; Gill, 1980).

The second stage of the large-scale tropical meteorology revolution was a series of observational papers. For example, Yanai and Mauryama (1966), Wallace and Kousky (1968), and many others identified most of the Matsuno and Longuet-Higgins modes as fundamental components of the low latitude tropospheric and stratospheric circulation.[1]

Recent studies have suggested that there may be another, very special, role for the very low frequency equatorial Kelvin wave. There is increasing evidence that the Madden–Julian oscillation (i.e., the 40–60 day mode) in the tropics, first described by Madden and Julian (1972), may be part of an adjusting stationary Kelvin wave through some form of internal feedback (e.g., Lau and Phillips, 1986).

b. *The role of stationary equatorially trapped fundamental modes in determining the mean state of the tropical atmosphere*

The concept that the *stationary* equatorial Kelvin wave plays a fundamental role in determining the mean state of the tropical atmosphere has been the result of considerable theoretical effort (e.g., Webster, 1972, 1973; Chang, 1977; Gill, 1980, etc.). Observational analyses by Krishnamurti (1971) showed that the large-scale mean structure of the tropical atmosphere possessed, what he termed, ". . . east–west circulations . . ." (later given the generic title of "Walker circulations"), centered on the equator with an amplitude that decreased exponentially towards the poles.

The Walker circulations were interpreted by Webster (1972, 1973) and Gill (1980) as stationary equatorial Kelvin waves forced within a generally westward equatorial flow. Chang (1977) showed that there had to be significant dissipation in order for the stationary modes to have the proper vertical scale. This is because the frequency of an inviscid Kelvin wave with a slow enough phase speed to have a zero Doppler shifted phase speed (thus producing a stationary solution) has a vertical scale that is an order of magnitude smaller than that observed. However, with dissipation rates matching cumulus mixing, a mode of a particular horizontal scale is stretched in the vertical to fill the depth of the troposphere (Chang, 1977).

Figure 1 shows a schematic view of the Walker Circulation along the equator for two sea-surface temperature distributions matching La Niña and El Niño conditions (Webster, 1983).[2] It is worth noting that the magnitude of the easterlies and westerlies exceed the magnitude of the zonally averaged mean easterly zonal current. Thus, the combination of the sea-surface temperature distribution and the location of the tropical continents, which together produce the form of the Walker Circulation, *introduce considerable longitudinal stretching deformation*[3] (referred to subsequently as longitudinal stretch) *into the mean tropical circulation.* For example, during the boreal fall and winter, the monthly averaged westerlies of the upper troposphere over the eastern Pacific Ocean exceed 10–20 m s^{-1} which introduce maximum longitudinal stretch along the equator. During the boreal summer or during Pacific Ocean warm episodes or El Niño periods, the equatorial longitudinal stretch diminishes over the Pa-

[1] Using FGGE winter MONEX data, Williams (1981) showed that there may be tropospheric counterparts to the stratospheric Kelvin modes (e.g., Wallace and Kousky, 1968). Williams showed that an eastward propagating Kelvin-like circulation feature along the equator appeared to be produced as a response to forcing by a cold surge from higher latitudes. Despite this intriguing diagnosis, there still appears to be limited evidence that the high-frequency *transient* Kelvin wave possesses a role in the tropical troposphere that matches the importance of its oceanographic counterpart as described, for example, by Mysak (1980). But elsewhere in the atmosphere the transient Kelvin wave appears to possess a substantial role that is more in keeping with its oceanic importance. P. J. Webster and J. M. Fritsch (personal communication) and subsequent work by P. J. Webster and D. Leathers (personal communication) have shown that, together with atmospheric shelf wave, the transient Kelvin wave explains a large part of the observed variance close to major orographic features.

[2] We use La Niña and El Niño as convenient terms to describe the extreme values of positive and negative Southern Oscillation Index, respectively, following Philander (1986).

[3] The shearing and stretching deformation fields of a horizontal flow are written traditionally as $(\bar{u}_y + \bar{v}_x)$ and $(\bar{u}_x - \bar{v}_y)$. Thus, for consistency, we must refer to the zonal variation of the zonal wind component (i.e., $\bar{u}_x$) as the longitudinal stretch of the flow and not, as it is often incorrectly called, the longitudinal shear. The longitudinal shear, of course, is given by $\bar{v}_x$.

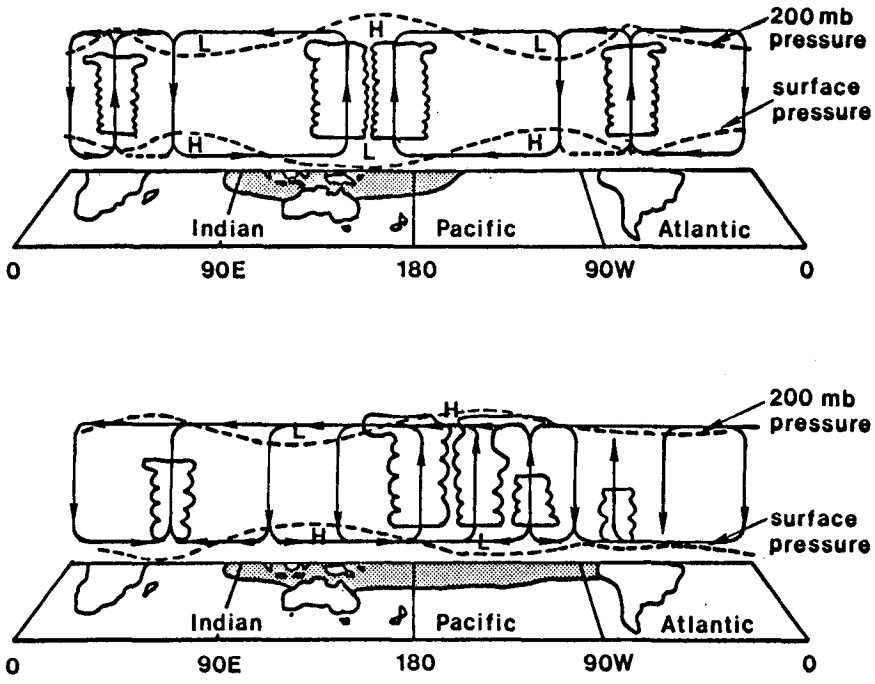

FIG. 1. Schematic view of the Walker Circulation along the equator during El Niño (lower panel) and La Niña (upper panel) periods that occur at the extremes of the Southern Oscillation. The shaded areas indicate sea surface temperatures warmer than 27°C and the dashed lines show relative horizontal pressure variations in the lower and upper troposphere. (From Webster, 1983)

cific Ocean region but increases over the Atlantic Ocean.

c. *Relationships between the tropical and the extratropical circulation*

Bjerknes (1969) noted that during El Niño periods, the anomalous tropical climate (see Fig. 1) appeared to be associated distinctly with variations in the circulation patterns in higher latitudes. A number of studies (e.g., Opsteegh and Van den Dool, 1980; Hoskins and Karoly, 1981; Webster, 1981) suggested that the influence of the perturbed tropics was transmitted as a train of Rossby waves from the anomalous heating regions. Webster (1982) argued that the transmission to higher latitudes would be most efficient towards the hemisphere where the westerlies were closest to the equator. This explained why the observed correlations between the tropics and the higher latitudes were strongest in the winter hemisphere.

However, the simple model of a train of waves emanating out of the anomalous heating region does not bear close scrutiny. Observational studies indicate a much more complicated relationship with a diversity of apparent wave train patterns. Also, modeling studies by Keshevamurty (1982) and Geisler et al. (1985), show a distinct insensitivity in the extratropical response to the location of the anomalous tropical heating. Similar phase locking of the high latitude response has been noted in diagnostic studies by Lau and Phillips (1986) with regard to the Madden and Julian oscillation irrespective of the location of the tropical convection. Furthermore, O'Lenic et al. (1985) found a similar insensitivity of equatorial forcing region to the phase of the extratropical response but on even shorter time scales.

Despite the problems noted here, there are some compelling arguments that suggest that the concept of an emanating Rossby wave train from the tropics is basically correct even if it is more complicated than originally perceived. There is, of course, the observed seasonality of the response at high latitudes that may be tied to the ability to generate wave trains more easily in the winter hemisphere (e.g., Webster, 1982). Furthermore, Hoskins and Karoly (1981) suggested that there should be strong scale dependency of the response with latitude due to given basic state distribution. Indeed, the anomalous climate at very high latitudes is found to be of a much larger spatial scale than in the middle latitudes, as predicted by Hoskins and Karoly.

Perhaps the greatest problem with the pure wave train teleconnection theory is that it does not take into account transient modes in a direct sense, especially in the tropics. Opsteegh and Van den Dool, 1980; Hoskins and Karoly, 1981; Webster, 1981, 1982 were all steady-state studies. Heating was assumed to be time independent and some sort of simple undefined aggregate of the transient modes.

d. The relationship between transients and the mean state of the tropical atmosphere

It is the mean state of the tropical atmosphere, with its slowly evolving shearing and stretching deformation fields created in the manner described here, that the transients within the tropics, or those propagating towards the tropics must contend. However, this full three-dimensional structure of the tropics has been largely ignored in terms of how it may affect the properties of transient or stationary modes or their propagation characteristics.

The role of *latitudinal* shear and its relationship to propagating synoptic and planetary scale disturbances has been understood for a considerable time. Charney (1969) showed that certain values of the mean wind should act as effective barriers to the equatorward propagation of extratropical disturbances. For transients of synoptic scale, the critical values of the mean wind are found to be weak and easterly. For stationary waves, the critical value of the zonal wind component is zero. Transient planetary scale extratropical waves possess critical latitudes where the wind speed is strong and easterly. These modes could be expected to propagate through the equatorial easterlies. However, Charney argued that they were of small amplitude and that their transmission was of little significance meteorologically. Charney's study emphasized the propagation of nondivergent extratropical modes *towards* the tropics through a *zonally averaged* basic state.

The study of the interaction of extratropical waves and shear flow was extended, in kind, by Webster and Holton (1982, hereafter referred to as WH), but with an emphasis on the equatorial longitudinal stretch and latitudinal shear discussed above. Noting the juxtaposition of the 200 mb equatorial westerlies and transient activity (defined here as the perturbation kinetic energy, $\overline{\text{PKE}}$) from analyses of Murakami and Unninayer (1977), WH suggested a new, distinct and important role for the equatorial westerlies. They posed and tested the hypothesis that the equatorial westerlies acted as a corridor, or a duct, for extratropical rotational modes. The regional maxima in $\overline{\text{PKE}}$, they reasoned, were the result of the deep propagation of disturbances into the tropics through the westerly duct. When the westerlies were either weak or nonexistent, such as during the boreal summer or during El Niño times, the extratropical waves were confined to the hemisphere of origin or because their meridional group speed depends upon the strength of the westerlies, which weaken during these periods, their energy dissipates before arriving in the tropics.

A number of studies have considered longitudinal variation of the time-mean basic state. Specifically, Simmons (1982), Branstator (1983) and (1985) considered a so-called "wavy-basic state." The latter study was aimed at interpreting the very long general circulation model simulations of Geisler, et al. (1985). While all studies have been very useful in understanding wave behavior in complex basic flows, they are restricted in their realism within the deep tropics where the divergent component of waves is strong. This is because the cited studies refer to a purely barotropic system. However, as we will develop in section 3, the nature of barotropic modes is very different than that of the divergent equatorially trapped modes. Specifically, the barotropic mode possesses a two-dimensional group speed (i.e., longitude and latitude) and is not different, qualitatively, from a barotropic rotational mode located anywhere on the globe. On the other hand, with divergence the modes become anisotropic in nature and emphasize their longitudinal phase and group speed components. Presumably, a free-surface barotropic model is a minimum requirement for the study of near-equatorial transient and stationary modes. The relevance of the WH paper was that it provided, for the first time, a physical significance to the tropical westerly regions. It also provided an explanation of why there may be local concentrations of transient energy along the equator.

e. Are there other source regions for the low latitude $\overline{\text{PKE}}$ maxima?

The colocation of the equatorial westerlies and the $\overline{\text{PKE}}$ maxima was reexamined by Arkin and Webster (1985) using a much longer NMC dataset than was available to Murakami and Unninayer (1977). They showed conclusively that the $\overline{\text{PKE}}$ within the equatorial westerlies was at least a factor of 2 or 3 larger than values within the easterlies, in agreement with the theoretical results of WH and their interpretations of the Murakami and Unninayer diagnostics. However, the study could not specifically confirm the hypothesis of WH regarding the origin of the transient energy, and, at best, could offer only evidence that was not inconsistent. The dataset was comprised of monthly mean variables and the fields of $\overline{\text{PKE}}$ were made up of the sum of variances of time scales less than one month. Arkin and Webster's failure emerges from the impossibility of recomposing the variance structure on submonthly time scales from their dataset in order to determine the transient's genesis regions or even their frequency spectra.

In summary, from an observational point of view, it is still an open question where the variance maximum in the equatorial westerlies originates. Certainly, WH offered one possible explanation, but is it unique? For example, is it possible that the variances originate, at least in part, from source regions located within the tropics?

f. Three criteria for the existence of tropical sources for the $\overline{\text{PKE}}$ maxima

Webster and Holton dismissed the possibility of the $\overline{\text{PKE}}$ maxima being driven by energy sources at low

latitudes. Their conclusion was based on the fact that the major convective regions, presumably source regions, are removed geographically from the equatorial westerlies. In fact, the westerlies themselves coincide with convective minima. This colocation can be seen in Fig. 2 where the mean boreal winter zonal wind field at 200 mb (upper panel), the mean outgoing longwave radiation field (middle) and the corresponding $\overline{PKE}$ field (bottom) are plotted relative to the same longitudinal axis along the equator. Clearly, the major convection coexists with the weak easterly regime. The $\overline{PKE}$ maxima, on the other hand, coincide with the stronger equatorial westerlies and the convective minima.

It would seem possible, though, under a certain set of circumstances, for energy sources within the tropics to create the $\overline{PKE}$ maximum, even with the geographic separation of source and transient energy maximum. However, these circumstances would require the satisfaction of *three criteria* relating to the mean state of the tropical atmosphere and of the equatorial modes existing within that mean state. Such criteria would be:

1) There must be physical processes that create transient energy within the tropics.

2) There must be a mechanism for the lateral transmission of energy from the energy source to the region of the apparent accumulation of energy; i.e., in the vicinity of the upper tropospheric westerlies.

3) There must be a means of accumulating the transmitted energy in the regions of equatorial westerlies.

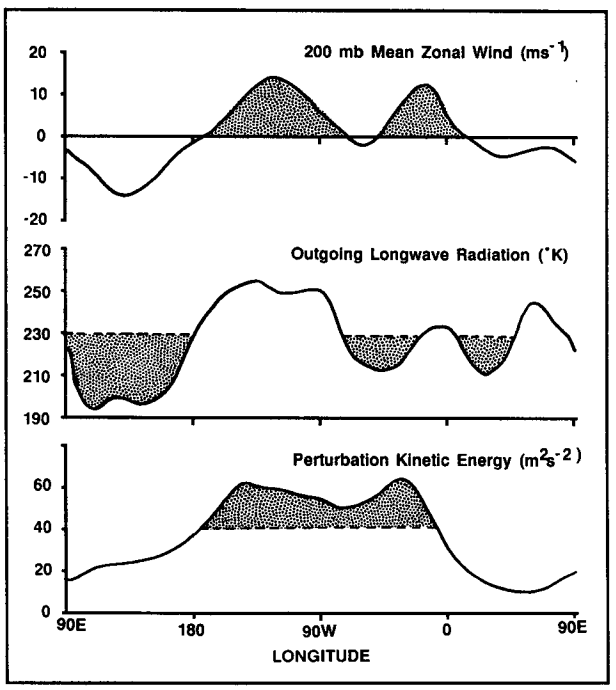

FIG. 2. The relative positions of the mean seasonal wind fields, the mean convection and the centers of transient action along the equator. These are represented by the mean zonal wind ($\bar{u}$, m s^{-1}, upper panel), the mean outgoing longwave radiation (OLR, °K, middle panel) and the perturbation kinetic energy field ($\overline{PKE}$, m^2 s^{-2}, lower panel). The fields represent mean boreal winter conditions except for the $\overline{PKE}$ field which is the mean field for December, January and February 1976–77. For ease of comparison, the regions of westerlies, of OLR < 230° and of values of $\overline{PKE}$ > 40 m^2 s^{-2} are shaded.

g. A hypothesis to satisfy the three criteria

Most certainly, criterion 1 is satisfied in the tropics. Figure 2 shows distinct regions of convective activity that are quite capable of exciting families of equatorially trapped modes over wide frequency and space scales (e.g., see Lim and Chang, 1983). However, whether or not these families of modes can account for the necessary energy propagation or for the energy accumulation (i.e., criteria 2 and 3) has yet to be shown. Most certainly, criterion 3 requires the development of new concepts.

In order to seek missing mechanisms, if indeed they do exist, we reemphasize that the existence of considerable longitudinal stretching deformation in the zonal wind component of the equatorial basic state has been ignored in most earlier studies of equatorially trapped mode characteristics. We assume here that longitudinal stretch possesses some importance and hypothesize that if equatorially trapped modes are capable of transmitting energy longitudinally from one region to another, thus satisfying criterion 2, then:

> *A convergence of the equatorially-trapped modes group characteristics will occur producing a regional wave energy accumulation zone in the vicinity of the equatorial westerlies if the longitudinal stretch is sufficient.*

If proved true, we would have provided a mechanism that would satisfy criterion 3. It is the testing of this hypothesis and the discussion of its implications that constitute the major thrust of our study.

In section 2 we will examine briefly the magnitude of the longitudinal stretch along the equator and the relative locations of the $\overline{PKE}$. In section 3 we will seek analytic solutions using WKBJ techniques to examine the impact of longitudinal stretching deformation on equatorial wave dynamics. The simple analytic techniques emphasize the longitudinal structure of the basic flow that modes with a longitudinal group speed contend. In its simplicity, it does not consider lateral propagation of modes or implications of a meridionally varying flow. Section 4 develops a more complete model where numerical techniques are used to study the propagation of transient equatorial waves through a nonlinear basic flow similar to the observed mean state of the tropical atmosphere. The basic flow in the numerical model contains both longitudinal and latitudinal stretching and shearing deformation fields which allow for the testing of its assumptions made in the previous simple analysis and discussed in subsequent sections. Section 8 contains a summary of the

results, together with some speculations relating to the application of the concepts developed in the paper.

2. Stretch structure of the tropical atmosphere

Both shearing and stretching deformation fields of considerable magnitude exist in the tropical atmosphere. Figure 3 shows a comparison of the 200 mb $\bar{u}_x$ field along the equator, 30°N and 30°S for January. The longitudinal stretch in the winter hemisphere (dashed) is largest by a factor of 2. However, the stretch at the equator (solid) is of the same magnitude as that in the Southern Hemisphere (dash-dotted). We note, for future reference, that along the equator there exist large regions of negative longitudinal stretch (shaded) to the east of the major westerly maxima.

Generally, in absolute terms $\partial\bar{u}/\partial y > \partial\bar{u}/\partial x$. However, when the shear and stretch are compared relative to the normalized longitudinal and latitudinal scales of the mode, X and Y, the inequality reverses; i.e., $\partial\bar{u}/\partial X > \partial\bar{u}/\partial Y$ because the longitudinal scale of the equatorially trapped mode is nearly an order of magnitude greater than the latitude scale (e.g., see Gill, 1982; Webster, 1983). Furthermore, the longitudinal stretch is in the direction of the zonal propagation of the trapped equatorial waves. Thus, although smaller in absolute magnitude than the latitude shear, we should explore, initially, the possible impact of the equatorial longitudinal stretch of the zonal flow on the behavior of the equatorially trapped waves. In the numerical studies described in sections 4–7, we will consider wave propagation in flow with full shearing and stretching deformation fields.

Figure 4 shows a longitude–time section of $\bar{u}$ and the $\overline{PKE}$ for a 15-year period. Mean seasonal values were used. The most notable features are the distinct regions of easterlies and westerlies that dominate the eastern and western hemisphere, respectively. The extremes of the Southern Oscillation, indicating El Niño and La Niña, are shown along the ordinate as x and y. During El Niño times the westerlies are weak in the Pacific Ocean with relatively small values of the $\overline{PKE}$. On the other hand, the Atlantic region possesses much stronger values of westerlies and transient kinetic energy. However, during La Niña the situation reverses. The $\overline{PKE}$ are the largest over the central and eastern Pacific Ocean and accompany very strong westerly winds. Only moderate westerly winds exist over the Atlantic Ocean.

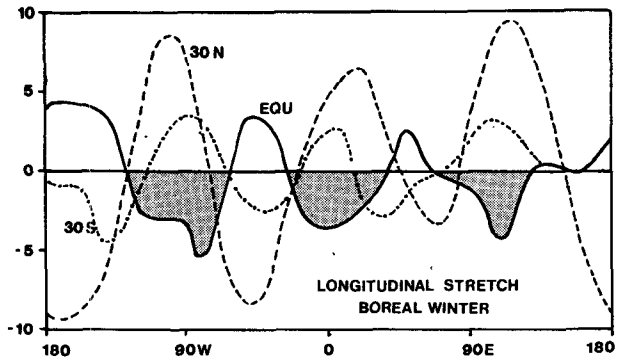

FIG. 3. Comparison of the longitudinal stretch of the mean zonal flow during the boreal winter at 30°N (dashed) 30°S (dash-dot) and the equator (solid). Units are m s^{-1}/1000 km. Regions of negative longitudinal stretch along the equator are shaded.

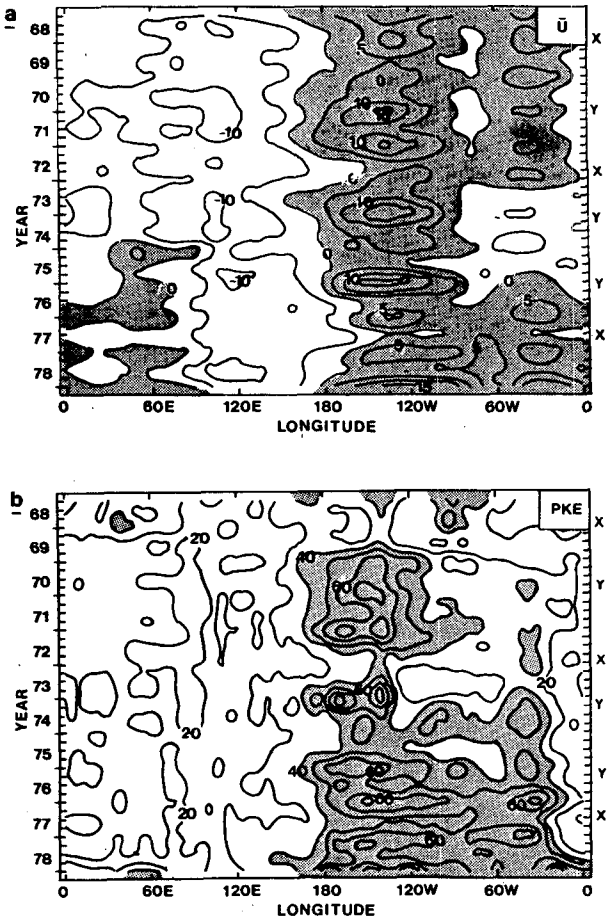

FIG. 4. Time–longitude section of the 200 mb mean zonal velocity component and the $\overline{PKE}$ along the equator over a 15-year period. El Niño and La Niña periods are labeled along the abscissa as x and y (after Arkin and Webster, 1985).

3. Identification of wave energy accumulation regions: Simple analytic solutions of equatorially trapped wave motion in a basic state with longitudinal stretch

Matsuno (1966) pointed out a fundamental difference between tropical and extratropical modes: the highly divergent structure of equatorial modes and the nondivergent structure of extratropical modes (see also, Lindzen, 1967; Webster, 1983 and, recently, Hendon, 1986). Thus, a natural starting point for the WKBJ examination of modes in complex basic flows near the equator would be with a model that reflects the divergent structure such as a free-surface (and, thus diver-

gent) barotropic model. However, at a later time we will wish to compare our results with purely barotropic interpretations of tropical flow (e.g., as emphasized by Simmons, 1982; Branstator, 1983, 1985). We will, therefore, develop both barotropic and divergent barotropic model structures simultaneously to facilitate later comparisons.

Traditionally, theoretical studies of both barotropic and divergent barotropic modes have been made relative to basic states at rest, in solid rotation or with very simple latitudinal shear. But, with the consideration of more realistic and complex basic flows that include, say, both shearing *and* stretching deformation, analytic tractability is rapidly lost. Thus, if we seek analytic solutions at all, we must be satisfied with either an extremely simple, and probably unrealistic, basic state or the approximations inherent in the WKBJ approach.

The WKBJ approximation is well known. With the scheme, it is assumed that the multidimensional coefficients of the inseparable system are locally constant assuring local separation. In the initial instance, one assumes that the time scales of the basic flow (here the slowly evolving Walker Circulations of Fig. 1) are very long as compared to the time scales of the transient modes under consideration. Thus $\bar{u}$ may be considered time independent relative to the time scales of the transients. Further, it is assumed that the spatial scale of the horizontal stretch of the basic field is large compared to the spatial scale of the transients. That is, we can also assume locally that $\bar{u}$ is spatially constant, again, relative to the spatial scale of the transients.

We should also be cognizant of the potential problems associated with the use of the WKBJ approach at low latitudes. As the equatorial transients possess very large longitudinal scales, it is conceivable that the WKBJ scale separation approximations may be overtaxed. However, with the appropriate caveats, we can at least anticipate some aspects of the behavior of equatorial modes in a variable basic flow and use this knowledge to develop a more complete model.

a. *Fundamental structures of barotropic and divergent-barotropic modes*

We consider a flow $\bar{u}(x)$, where x represents the eastward direction, and we make the assumption that there is sufficiently large spatial separation between the scale variation of the horizontal stretch and the scale of the transient mode. That is, we are assuming that the change of $\bar{u}$ is gradual over the scale of a wavelength. The local Doppler shifted frequency ω_d can be written as (e.g., Lighthill, 1978; Gill, 1982):

$$\omega_d = \bar{u}k + \omega_r \tag{1}$$

where k is the zonal wavenumber and ω_r the modal frequency in a frame of reference where $\bar{u} = 0$ locally.

A free surface fluid analogue to an atmosphere on an equatorial β-plane, assuming locally that $\bar{u}$ is a constant, can be written as

$$u_t + \bar{u}u_x - \beta yv + gh_x = 0 \tag{2}$$

$$v_t + \bar{u}v_x + \beta yu + gh_y = 0 \tag{3}$$

$$h_t + H_0(u_x + v_y) + \bar{u}h_x = 0 \tag{4}$$

where H_0 is the mean depth of the fluid and h, u and v are the perturbation height and velocity components. We note from (4) that this general form allows for divergence depending upon the scale of H_0.

If we now assume that $\bar{u}$ is locally constant relative to the scales of the perturbation, we can assume solutions of the form

$$u, v, gh(x, y, t) = \tilde{u}, \tilde{v}, \tilde{h}(y) \exp i(kx - \omega_d t). \tag{5}$$

With (5) and (2)–(4) we can obtain an equation in $\tilde{v}(y)$ after the elimination of $\tilde{u}$ and $\tilde{h}$. This is

$$\tilde{v}_{yy} + \left\{\frac{(\omega_d - \bar{u}k)^2}{c^2} - k^2 + \frac{\beta k}{(\omega_d - \bar{u}k)} - \frac{\beta^2}{c^2} y^2\right\}\tilde{v} = 0, \tag{6}$$

where $c = \sqrt{gH_0}$. We note that (6) takes on very different characteristics depending on the magnitude of c. If c is very large, corresponding to a very deep system, then the system is purely barotropic and, from (4), nondivergent. In this case, (6) becomes an isotropic wave equation,

$$\tilde{v}_{yy} + \left\{-k^2 + \frac{\beta k}{\omega_d - \bar{u}k}\right\}\tilde{v} = 0, \tag{7}$$

which possesses solutions of the form,

$$\tilde{v}(y)\alpha e^{ily}, \tag{8}$$

or using (5)

$$v(y)\alpha \exp i(kx + ly - \omega_d t), \tag{9}$$

if

$$\omega_d = \bar{u}k - \frac{\beta k}{k^2 + l^2}. \tag{10}$$

These modes possess wave forms in both x and y and possess nonzero group speeds:

$$C_{gx} = \bar{u} - \frac{\beta(l^2 - k^2)}{(k^2 + l^2)^2} \tag{11}$$

$$C_{gy} = \frac{2\beta kl}{(k^2 + l^2)^2}. \tag{12}$$

Clearly, the purely barotropic Rossby wave possesses a structure that is characteristic of *any* β-plane on the globe. That is, the nondivergent Rossby wave at the equator is no different than an extratropical Rossby wave except for a larger β. Furthermore, the modes are not, in general, trapped about the equator. For trapping to occur, $C_g(y)$ in (12) must be zero which can only occur if $l = 0$. Thus, from (12),

$$C_{gx}(l = 0) = \bar{u} + \frac{\beta}{k^2} \tag{13}$$

with the group speed being a monotonic function of k. We should note, though, that even this mode is common to all β-planes irrespective of latitude!

On the other hand, for smaller values of c, so that in (4) the system is more strongly divergent, the entire modal structure changes with distinct equatorial characteristics with forms that are horizontally anisotropic. Setting $\eta^2 = c_1^{1/2}y$ where $c_1 = \beta^2/c^2$ changes (6) to the form

$$\tilde{v}_{\eta\eta} + \left\{\left[\frac{(\omega_d^2 - \bar{u}k)^2}{c^2} - k^2 + \frac{\beta k}{(\omega_d - \bar{u}k)}\right]\frac{c}{\beta} - \eta^2\right\}\tilde{v} = 0 \tag{14}$$

which has solutions of the form [with (5)]

$$v = Ae^{-\eta 1/2}H_n(\eta)e^{i(kx-\omega_d t)} \tag{15}$$

where $H_n(\eta)$ are Hermite polynomials and n is a latitudinal nodal number. With the allowance for divergence, the waves now take on a character that is unique to the equatorial β-plane. The solutions to (14) are equatorially trapped and thus possess a horizontal group velocity which has a strong zonal component along the equator. For the two principal low-frequency modes we will consider, the equatorial Rossby wave and the Kelvin wave, we can write the dispersion relationships from (4) (e.g., Gill, 1982) as

$$\omega_d = \bar{u}k - \beta k/\{k^2 + \beta(2n + 1)/c\} \tag{16}$$

$$\omega_d = \bar{u}k + ck, \tag{17}$$

respectively. Using (1), (16) and (17), we can obtain expressions for the local Doppler shifted phase and group speeds:

$$C_{pd} = \bar{u} + \omega_r/k = \bar{u} - \beta/\{k^2 + \beta(2n + 1)/c\} \tag{18}$$

$$C_{gd} = \bar{u} - \{\beta(k^2 + \beta(2n + 1)/c) - 2k^2\beta\}/(k^2 + \beta(2n + 1)/c)^2 \tag{19}$$

for the Rossby wave, and

$$C_{pd} = \bar{u} + c \tag{20}$$

$$C_{gd} = \bar{u} + c \tag{21}$$

for the Kelvin wave. In (18)–(21) because of the absence of meridional components, we have omitted the component designation of the phase and group speeds.

It is clear from (20) and (21) that the Kelvin wave is nondispersive for all scales of motion. That is, energy associated with the wave will move eastward from a source at a constant group speed which is identical to the phase speed. On the other hand, (18) and (19) indicate that the equatorially trapped Rossby wave is only approximately nondispersive for very large longitudinal scales of motion, i.e., for large scales relative to a stationary basic state, wave energy will move westward away from a source with a local group speed that is similar to the Rossby phase speed. However, as k increases, it can be seen that, although $C_p < 0$ for all scales, C_g becomes >0. Relative phase and group speeds for a number of modes are shown in Fig. 6 and discussed in detail in section 3b.

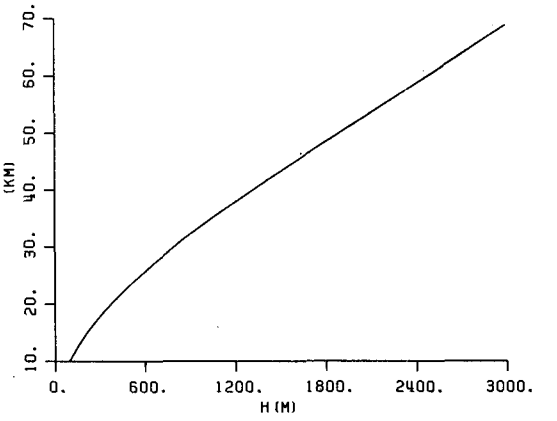

FIG. 5. Relationship between the vertical wavelength (L_z, km) and the equivalent depth (H_0, m).

Equations (18)–(21) also indicate that the phase and group speeds are functions of the fluid depth H_0. As shown for equatorial waves by Matsuno (1966), Lindzen (1967) and Longuet-Higgins (1968), the depth H_0 can be interpreted as the equivalent depth of one vertical mode of the real atmosphere and thus to a vertical length scale.[4] Lindzen (1967) showed that for an isothermal atmosphere of temperature T_0, without vertical shear, the relationship between a vertical wavelength L_z and the equivalent depth H is

$$L_z = 2\pi/\{\gamma/(\Gamma h_s H_0) - 1/(4h_s^2)\}^{1/2} \tag{22}$$

where $h_s = RT_0/g$, $\Gamma = C_p/C_v$ and $\gamma = (\Gamma - 1)/\Gamma$. The relationship between L_z and the depth H_0 is plotted in Fig. 5. Clearly, for half wavelengths or wavelengths that are confined within the troposphere, we can establish a meteorologically significant range for H_0 of $\leqslant$2000 m (see Holton, 1976; Webster and Holton, 1982; Webster, 1983).[5]

b. *Local phase and group speeds relative to the observed winds at low latitudes*

Plots of the local phase and group speeds of the free-surface barotropic equatorially trapped Rossby wave, as a function of equivalent depth, for nodal numbers n = 1 and 3 are shown in Fig. 6a, b for longitudinal

[4] Formally, H_0 appears as the principal component of separation coefficient in the separation of the vertical and horizontal parts of the linear primitive equations written for an atmosphere either at rest or in solid rotation. However, separability is lost if there is vertical shear. A complete development is given in Holton (1976).

[5] In the analytic development of this section and in the numerical results shown in section 7 the results refer mainly to a rather deep equivalent depth of H_0 = 2000 m. The choice of H_0 is in order to facilitate a comparison of the results with those of WH. However, the results will be shown to be rather robust over a much wider range of H_0 as indicated in Figs. 8a, 9c and 25.

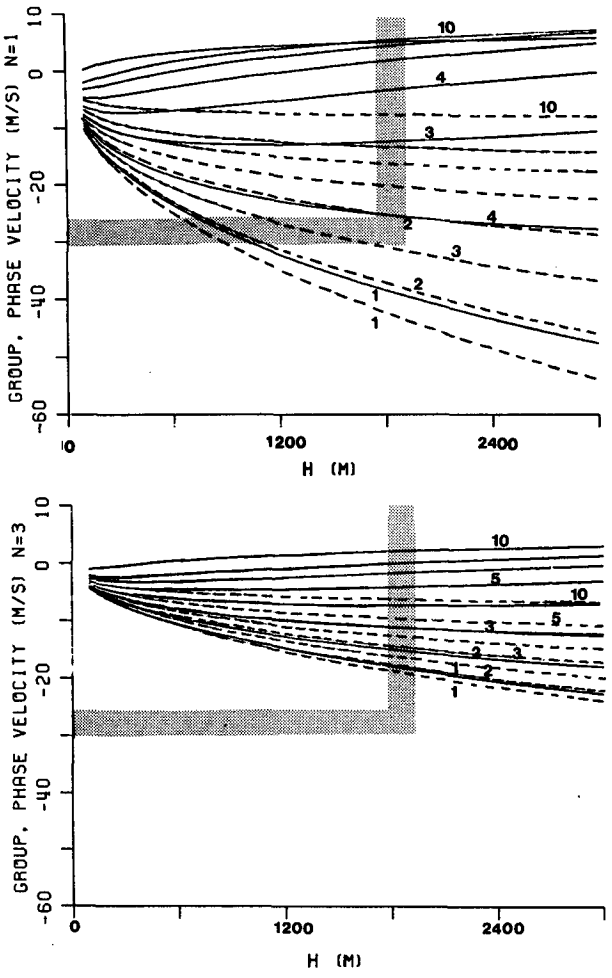

FIG. 6. Plots of the local phase (dashed lines) and group speeds (solid) for modes $n = 1$ (a) and $n = 3$ (b) as a function of equivalent depth H_0 (m) for longitudinal wavenumbers $k = 1, 2, \cdots, 7, 10$. The shaded bars enclose the limits of the observed wind fields shown in Fig. 4.

wave numbers $k = 1$–7 and $k = 10$. Generally, C_p increases as H_0 but decreases rapidly as k. The nondispersive nature of the large-scale Rossby waves can be seen by comparing the phase and group speeds. The character of C_p follows C_g for small k but decreases rapidly for $k > 5$. For $k = 10$, the group speed is weak and westerly. The same characteristics are apparent for $n = 3$, but both phase and group speeds are reduced by a substantial factor and the dependency on H_0 is diminished.

Figure 7 summarizes the group speed structure as a function of k for the family of Rossby waves $n = 1, 2, \cdots, 5$ with $H_0 = 2000$ m. The diagram shows a clear demarcation between the westward group speeds for large longitudinal scales and eastward for smaller scales. As n increases, the longitudinal scale at which the group speed changes sign decreases.

The shaded horizontal bars in Fig. 6a, b represent the limits of the observed mean equatorial westerlies (cf. Fig. 4) with which we can compare the local values of C_p and C_g for the Rossby wave. Similar comparisons, but with easterlies of similar values (see Fig. 4) can be made for the Kelvin wave using expressions (20) and (21). The following conclusions can be reached:

(i) Except for very small equivalent depths (say $H_0 < 100$ m or eqivalently, $L_z < 10$ km), the local Kelvin wave always moves eastward relative to a realistic basic state. Thus, for the inviscid Kelvin wave, both C_{gd} and C_{pd} are always positive, except for very small H_0.

(ii) The local Rossby wave Doppler phase and group speeds possess zero relative to the observed wind over a wide spectrum of scales. For $n = 1$ the gravest modes possess zeros for reasonable values of H_0. The slower values of C_{gd} corresponding to the small H_0 create local zeros within the observed wind envelope. The scale range for which $C_{gd} = 0$ increases substantially for all H_0 as we increase n.

Inferences (i) and (ii) refer to the *local* Doppler shifted group and phase speeds, i.e., they are true for a particular value of $\bar{u}$ for a mode of a particular scale k. However, we cannot, as yet, determine where the zeroes in C_{gd} and C_{pd} are because in the system we consider, k cannot remain constant, for a particular wave, within a basic flow $\bar{u}(x)$ that is time invariant.

The variation of k for a particular mode propagating through a longitudinally varying basic flow arises because $\bar{u}$ is a spatial function only. This implies that the coefficients of (2)–(4) are only spatial functions so that the Doppler-shifted frequency of a wave along a ray path must be constant. From (1) for a westward propagating Rossby wave, this is accomplished by k varying inversely with $\bar{u}_x(x)$ along the ray path. Thus, in regions where $\bar{u}$ decreases (i.e., $\bar{u}_x < 0$), the value of k must increase and the longitudinal wave length decrease. On

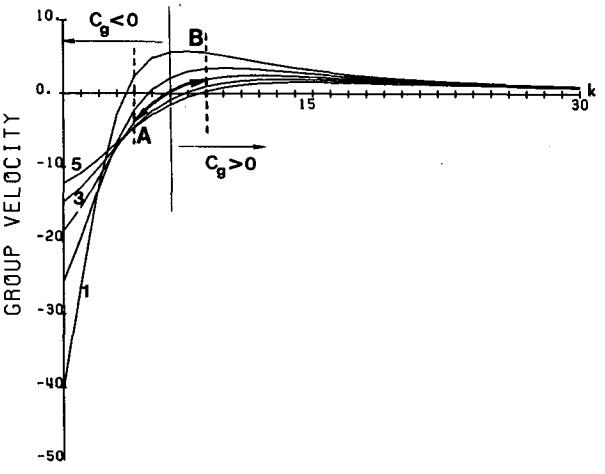

FIG. 7. The group velocity of equatorially trapped Rossby waves for $n = 1, 2, \cdots, 5$ and $H = 2000$ m. The line perpendicular to the abscissa at $k = 6$ demarks the $C_g = 0$ point for the $n = 3$ mode. Regions of negative and positive group speed are noted. The points A and B are referred to in the text.

the other hand, where $\bar{u}_x > 0$, k decreases and the scale increases. From (16) ω_r changes along the ray due to its functional dependence on k so that the two terms on the right-hand side of (1) conspire to produce a constant ω_d. From Lighthill (1978), it can be shown using (16) (see Appendix) that the governing equation for the change of k following a ray of equatorially trapped mode in a time-invariant basic flow is

$$\frac{dk}{dt} = \frac{\partial k}{\partial t} + \left(\bar{u} + \frac{\partial \omega_r}{\partial k}\right)\frac{\partial k}{\partial x} = -k\frac{d\bar{u}}{dx} \tag{23}$$

which substantiates the physical argument presented here.

A useful interpretation of Fig. 7 can be made using (23). Consider, say, the $n = 3$ mode. The vertical line at $k = 6$ shows the scale at which the group speed is zero. However, a $k = 4$ mode (A) has a westward group speed, whereas the $k = 8$ mode (B) possesses an eastward group speed. From (23) we can see that a $k = 4$ mode will move towards smaller scales and thus less westward group speeds if the stretch of the basic field is negative. On the other hand, a smaller mode moving into a region of positive stretch will grow to longer scale and develop a less eastward group speed. Thus, between Fig. 7 and Eq. (23) it is apparent that *the group speed of an equatorially trapped mode, regardless of the initial scale of the mode, will depend upon the sign of the stretch of basic flow. Indeed, the sign of the group speed may so change along a ray to create local zeros in the group velocity.*

From the foregoing discussion, it is clear that the zonally varying basic state has two distinct effects on the equatorial Rossby wave's phase and group speed. The first is the advection of the Doppler shifting of the Rossby wave group and phase speed by the local wind $\bar{u}$ such as would occur in a *uniform* basic state of arbitrary $\bar{u}$. The second effect is the more subtle change of the zonal wavenumber as the wave passes through the $\bar{u}(x)$ via (23) with the consequent change in the phase and group speeds through (18) and (19). Thus, in the strong stretch flow that exists along the equator (see section 2), we can expect significant variations in k, C_p and C_g of a wave emanating from an equatorial energy source, i.e., the two effects are not independent.

c. *Significance of the existence of longitudinal group speed zeros*

The existence of zeros in the Doppler shifted group speed appears to be of critical importance. For a slowly varying basic state, Whitham (1965) and Bretherton and Garrett (1968) showed that the wave action density, $\xi = \epsilon/\omega_r$, is conserved following a ray. The ϵ is the energy density of the wave defined by $\rho g h^2/2$, i.e.,

$$\partial \xi/\partial t + \partial(C_{gd}\xi)/\partial x = 0$$

or

$$\partial \xi/\partial t + C_{gd}\partial \xi/\partial x = -\xi \partial C_{gd}/\partial x. \tag{24}$$

For equatorially trapped Rossby waves and Kelvin waves, ω_r and C_g do not depend explicitly on x and t within the confines of the WKBJ approximations. Thus (24) may be written, using (19), as

$$\partial \epsilon/\partial t + C_{gd}\partial \epsilon/\partial x = -\epsilon d\bar{u}/dx. \tag{25}$$

Through (25) the impact of longitudinal stretch on the wave action density is quite clear. If the longitudinal stretch is sufficient to modify the Doppler shifted group speeds to produce zeros [see Fig. 7 and Eq. (23)], then there must be a region where ϵ will increase due to energy density convergence along a ray. From (25), we can predict that the local value of ϵ will wax and wane relative to the stretch structure of the basic flow. Only in the region where $\bar{u}_x < 0$ can the C_{gd} of the equatorial Rossby waves possess zeros. Furthermore, given the possibility of a zero in the group speed, the value of ϵ can grow exponentially with time in a particular region which, again for an equatorially trapped Rossby wave, must be in the negative stretch region. We will refer to these regions as *wave energy accumulation regions.*

From (25) we can anticipate that the maximum convergence of ϵ will occur where the criteria $\bar{u}_x|_{\max} < 0$. With a simple sinusoidal basic state, maximum wave energy accumulation will occur in the vicinity of $\bar{u} = 0$ on the *eastern* side of the westerly maximum.

d. *Ray paths in longitudinally varying flow along the equator*

The existence of wave energy accumulation regions along the equator can be illustrated using ray tracing techniques. The kinematic wave theory (e.g., Lighthill, 1978; Gill, 1982; Hoskins and Karoly, 1981; Karoly, 1983) gives the path of a ray as

$$dx/dt = C_{gd}. \tag{26}$$

Figure 8 shows the wave characteristics for various families of waves created at a variety of source points (A, B, . . ., F) spaced 60° of longitude apart along the equator within a zonal basic flow with easterlies and westerlies amplitude of 5 m s^{-1} ($\bar{u}$, upper panel). Plotted with the $\bar{u}$ curves are the local group speeds of the various modes. The curves on the middle diagram of each figure represent the local wavenumber of the wave along the ray path from (23). The actual ray paths are shown in the lower panel as a function of longitude and time for a 40-day period. A value of $H_0 = 2000$ m has been adopted although plots for modes starting at point B for $H_0 = 1000$, 500 and 100 m are shown in Fig. 8a for comparative purposes. For $H_0 = 2000$ m the propagation speed of the Kelvin wave is so rapid that the basic flow hardly affects its characteristics. Consequently, we have not included the Kelvin wave in Fig. 8. Figure 8b, c show similar characteristics for the (3, 2) and the (3, 3) modes, respectively. The plots for smaller values of H_0 in 8a indicate that the local accumulation phenomena exists over a wide range of equivalent depth.

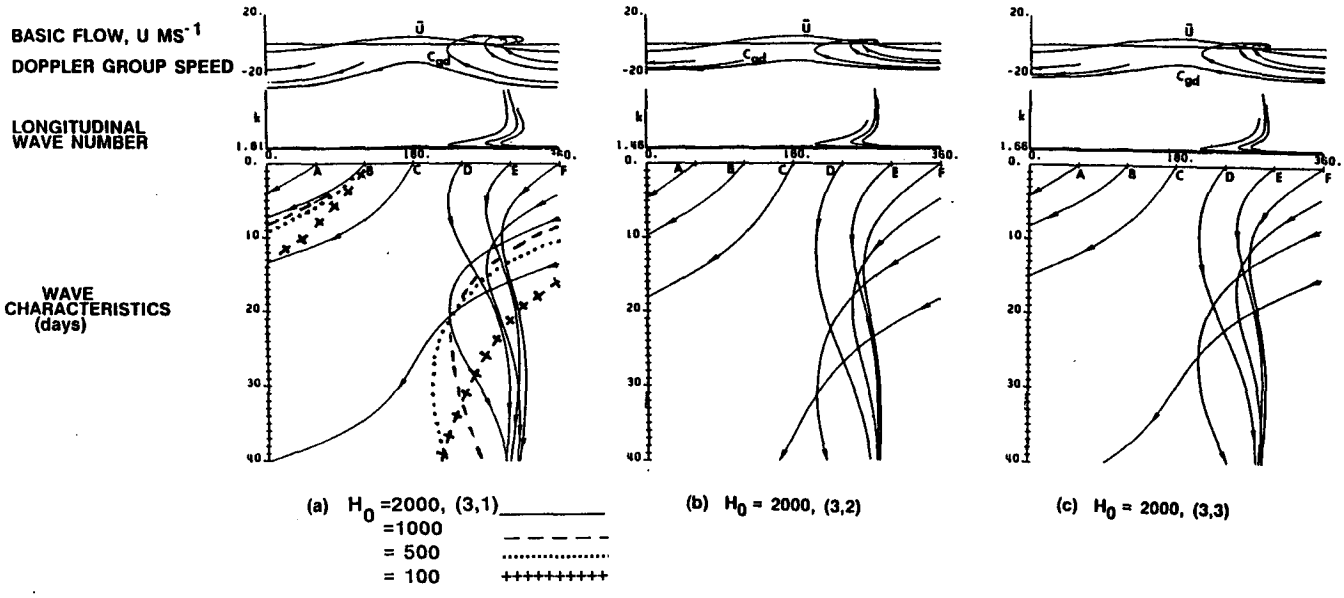

FIG. 8. The wave characteristics of various families of waves created at source points A, B, . . . , F along the equator for (a) the $k = 3$, $n = 1$ (3, 1) mode, (b), the (3, 2) mode and (c) the (3, 3) mode. The lower panel is a time–longitude plot of the ray paths. The Doppler shifted group speed relative to the basic state $\bar{u}$ is shown in the upper panel. The simple basic state has extremes of 5 m s^{-1}. The center panel shows the local longitudinal wavenumber along the ray path. The equivalent depth is 2000 m. Characteristics for (3, 1) modes with H_0 set at 1000, 500 and 100 m with the source point at B are shown in (a) as dashed, dotted and crossed lines, respectively.

Following the progress of a mode forced, say, at A (longitude 60°), we note an initial westward propagation of the wave. This occurs because, locally, the initial group speed of the mode and the basic flow are of the same sign. Given that there has to be a constant frequency constraint along a ray, according to kinematic wave theory (see section 3b), we see within the easterly regime that the wavelength is slightly longer than that at which it is forced. As the mode propagates westward through the longitudinal stretch flow the wavelength starts to decrease rapidly according to (23). With the change in wavelength, there is a corresponding change in group speed, as shown in Fig. 7. In turn, as the group speed decreases, the wavelength must decrease to maintain a constant frequency and, in this manner, a zero is approached in C_{gd}. Waves forced at other regions in the flow possess very different characteristics. For example, modes emanating from locations D and E find themselves in an environment that immediately places their Doppler shifted group speed near zero.

With the one exception (see section 3e), all modes in Fig. 8 eventually possess zeros in their Doppler shifted group speeds; i.e., all modes have wave energy accumulation regions for the given basic flow along the equator. The surprising aspect of the simple WKBJ solutions is that the wave energy accumulation regions for *each* family of modes occur in the same longitude belt, i.e., to the east of the westerly maximum where the stretch is maximum as indicated in (25). In the simple flow we consider here, this occurs where $\bar{u} = 0$.

Figure 9a, b shows two further examples of wave characteristics. Figure 9a refers to (6, 1) mode in the same simple trigonometric basic state. Figure 9b refers to the (3, 1) mode but forced in a stronger flow with extremes of ± 10 m s^{-1}. From Fig. 7 it is apparent that the initial group speed of the (6, 1) mode will be of moderate magnitude and towards the west. However, despite the differences in the modal numbers and their inherent differences in characteristics, the longitudinal stretch in the basic flow is such as to modify their behavior to form wave energy accumulation regions in similar longitudinal zones.

Figure 9c shows a case where the equivalent depth is very shallow ($H_0 = 100$ m) with a very strong basic state. Under these circumstances, the Kelvin wave (K) is modified significantly by the basic flow as $\sqrt{gH_0} \approx \bar{u}$ and forms an accumulation region in the strong easterlies. We note, though, that the Rossby mode still possesses an accumulation zone in the same region.

e. *The special untrapped mode*

In Figs. 8 and 9, there appears an anomalous mode originating at point C that does not appear to possess C_{gd} zeros, is not longitudinally trapped and hence propagates completely around the equator. Such characteristics can occur only if the group speed of the mode is sufficiently easterly so that $C_g - \bar{u} < 0$ at the westerly maximum of the basic flow or sufficiently westerly so that $C_g - \bar{u} > 0$ at the easterly maximum. Noting the strength of the basic state and the magnitude of the longitudinal group speeds (Figs. 6 and 7), it is obvious that only the longer scale equatorially trapped Rossby waves can satisfy the $C_g - \bar{u} < 0$ criteria. For the shorter

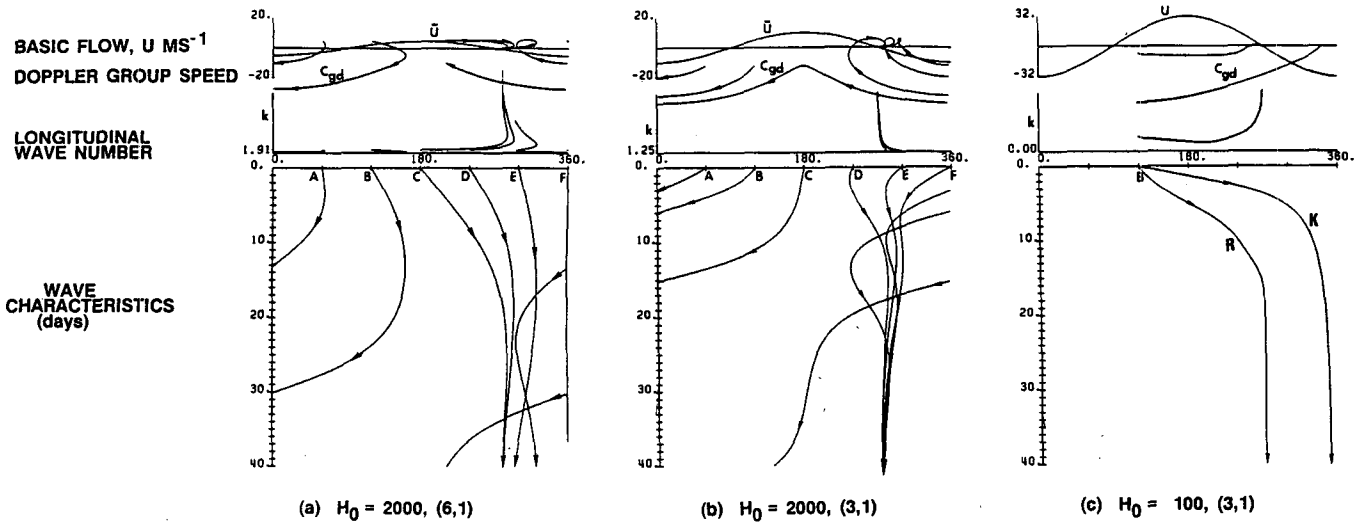

FIG. 9. As in Fig. 8a except for the (6, 1) mode, (b) the (3, 1) mode in a stronger basic state with extremes of ± 10 m s^{-1}, and (c) the (3, 1) Rossby mode (R) and the Kelvin mode (K) in a very strong basic state with extremes of ± 30 m s^{-1}. The equivalent depth is 100 m.

scale Rossby waves $C_g \ll \bar{u}$ near the easterly maximum so that $C_g - \bar{u} \ll 0$ within the basic state easterlies. Only the transient Kelvin wave can pass through the strong easterlies.

It is an interesting exercise to calculate what scale of Rossby waves, starting off at an arbitrary location along the equator, will just pass, untrapped, through a westerly maximum of arbitrary amplitude. For simplicity we assume that the basic state, $\bar{u}$, is given as a simple trigonmetric function along the equator with a maximum westerly magnitude $\bar{u}_0$ located at $x = 0$. Using (19), we seek the maximum value of k (i.e., k_0) for which $C_{gd} = 0$ at $x = 0$. That is, from (19) we have

$$\bar{u}_0 k^4 + \left[\frac{2\bar{u}_0\beta(2n+1)}{c} + \beta\right]k^2 + \frac{\bar{u}_0\beta^2(2n+1)^2}{c^2} - \frac{\beta(2n+1)}{c} = 0. \quad (27)$$

The k_0 is sought as it is this mode that will possess that slowest westward group speed that will just pass through the westerly maximum; i.e., so that $C_g - \bar{u} \leqslant 0$ at $x = 0$. All modes for which $k < k_0$ will pass through $\bar{u}_0$ as $C_g - \bar{u}_0 < 0$ (see Fig. 7). Equations (23) and (26) combine to give

$$\frac{dk}{dx} = -\frac{k(\partial\bar{u}/\partial x)}{C_{gd}}. \quad (28)$$

Using the limiting value k_0, for a given n, and $\bar{u}_0$ from (27) as an initial condition, we can use (28), together with (19), to obtain values of k at all x for specific basic states defined by the value of the westerly maximum, $\bar{u}_0$, and for various values of n.

Figure 10 plots the k loci for various $\bar{u}_0$ and $n = 3$ as a function of longitude. The intercept of the $\bar{u}_0$ curves and the ordinate occurs at $k = k_0$. The $\bar{u}_0$ curve defines the locus for all waves along the equator which will change their wavenumbers, in moving through the $\bar{u}_0$ basic state, to k_0 by the time they reach $x = 0$. For $\bar{u}_0 = 5$ m s^{-1}, for example, $k_0 = 3.7$. Following the $\bar{u}_0 = 5$ curve, we can see that all waves with $k < 2.2$ originating at x_2 will be untrapped. However, all $k > 2.2$ will be trapped as by the time they will have propagated westward and reach $x = 0$ their wavelength will have decreased beyond the critical value such that $k > k_0$. Similarly, waves originating at x_1, will be untrapped by the $\bar{u}_0 = 5$ basic flow if $k < 3$, but trapped if $k > 3$.

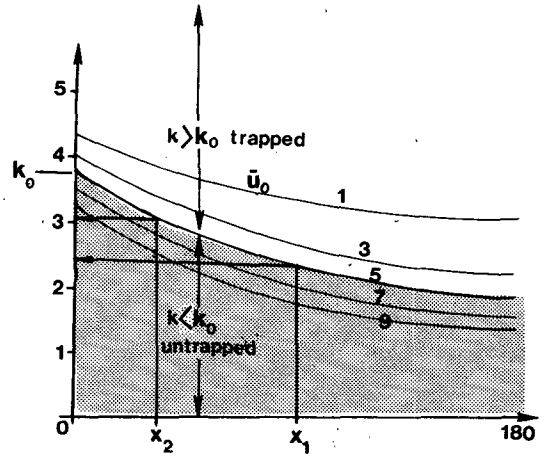

FIG. 10. The loci of k as a function of longitude for various trigonometric basic states with maximum westerly amplitude $\bar{u}_0$. Intercept of the $\bar{u}_0$ curves with the ordinate defines the maximum longitudinal wavenumber [k_0 obtained from a maximized (27)] that can just propagate through the westerly maximum. Intercepts with the $\bar{u}_0 = 5$ m s^{-1} curve at longitudes x_1 and x_2 show the scale of those waves that would just pass through a westerly maximum of 5 m s^{-1} if they were to originate from x_1 and x_2, respectively.

f. Perspective

In the previous discussion, we have obtained the characteristics of the equatorially trapped Rossby and Kelvin waves by using wave action conservation theory and ray tracing. These techniques, of course, are subject to considerable theoretical constraints. However, we have, at this stage, a strong suggestion of a physically reasonable mechanism of concentrating energy in a specific region of the tropical atmosphere; i.e., we may have found a property of the tropical atmosphere that satisfies criterion 3 discussed in the Introduction.

In fairness, it must be stated that the physical constraints inherent in our WKBJ approximations are severe. Yet, by considering a free-surface barotropic model, and thus retaining divergence structure, we are fairly certain that we are at least considering the appropriate physical modes; i.e., we have considered equatorially trapped modes that would not be apparent in a purely barotropic system. However, in the next section we will develop a model that is less dependent on limiting assumptions in order to test the robustness of the WKBJ results. Furthermore, the development of a more complete model will allow us to study linkages between the tropical accumulation regions and the circulation at higher latitudes.

4. The numerical model

To overcome the very obvious scale separation problems that exist with the WKBJ approximations, we will now develop a numerical model that can handle wave propagation through an inhomogeneous basic flow *without* scale separation approximations. The model we use is the free surface barotropic model of WH. Although numerical eigenvalue-eigenfunction techniques could be employed to find the solutions to the steady linear problem, we prefer to utilize a numerical initial value technique in order to study the evolution of the equatorial response to a transient equatorial forcing function within very complicated basic flows.

a. Model structure

Following WH, the momentum and continuity equations may be written in Mercator coordinates as

$$u_t - fv + I(u) = -gmH_x - \alpha u, \tag{29}$$

$$v_t + fu + I(v) = -gmH_y - \alpha v, \tag{30}$$

$$H_t + I(H) = M, \tag{31}$$

where the I are the nonlinear operators

$$I(u) = m(uu_x + vu_y), \tag{32}$$

$$I(v) = m(uv_x + vv_y), \tag{33}$$

$$I(H) = m\{(uH)_x + (vH)_y\} - Hvm_y. \tag{34}$$

The m is the Mercator map factor $\mathrm{sech}(\phi)$ where ϕ represents latitude; H represents the depth of the fluid that can be resolved into a mean depth H_0 and a deviation about the mean $h(x, y, t)$ such that

$$H = H_0(y) + h(x, y, t). \tag{35}$$

The $M(x, y, t)$ is a specified mass source–sink function which will be used to develop a specific basic flow; it also acts as the transient energy source; u and v represent the eastward and northward components of velocity, and mechanical dissipation is given by a Rayleigh friction with a rate coefficient α. A value representative of a 10-day dissipative time scale is chosen.

Equations (29)–(35) represent the full nonlinear model. A companion linear system can be created about an arbitrary nonlinear two-dimensional basic state $\bar{u}$, $\bar{v}$ and $\bar{h}$ where the dependent variables have been decomposed as

$$u(x, y, t) = \bar{u}(x, y) + u'(x, y, t) \tag{36}$$

$$v(x, y, t) = \bar{v}(x, y) + v'(x, y, t) \tag{37}$$

$$h(x, y, t) = \bar{h}(x, y) + h'(x, y, t). \tag{38}$$

Correspondingly, the I-functions may be linearized to the form

$$I'(u) = m\{\bar{u}u'_x + u'\bar{u}_x + \bar{v}u'_y + v'\bar{u}_y\} \tag{39}$$

$$I'(v) = m\{u'\bar{v}_x + \bar{u}v'_x + \bar{v}v'_y + v'\bar{v}_y\} \tag{40}$$

$$I'(H) = m\{(\bar{u}h')_x + \bar{v}(h')_y + H_0(u'_x + v'_y)\} - m_y(H_0v' + h'\bar{v}). \tag{41}$$

Thus, both linear and nonlinear versions of the model exist. In this initial instance, we will consider linear perturbations, using the model (29)–(31) with definitions of the I-functions given by (39)–(41) about the nonlinear basic state created by the fully nonlinear model (29)–(31), using the I-functions (32)–(34).

b. Method of solution

Both the linear and nonlinear versions of the model use the method of solution described in great detail by WH. A semispectral representation is employed. The variables are expanded in sines and cosines while a grid-point representation is used in latitude. The nonlinear terms (the I-functions (32)–(34)] or the nonhomogeneous linear terms that emerge from the linearization of the I-functions (i.e., the I'-functions) are evaluated using the transform method of Orzag (1970). This technique uses an exact grid representation of the Fourier coefficient recomposition. On this grid the I- and I'-functions are computed efficiently and exactly in grid space. These terms are then expanded in longitudinal eigenfunctions. Using the semi-implicit time differencing scheme of Holton (1976) and a staggered space-difference scheme in latitude, sets of linear simultaneous equations evolve that are readily solved by matrix inversion. Thus, the method of solution is

identical for either the nonlinear or linear sets described above.

c. Generation of the nonlinear basic states

It is necessary to generate basic states that are similar in character to the observed flow. This is accomplished by dividing the flow into zonally symmetric and asymmetric components. In (35) we can write

$$H_0(y) = H_{00} + H_b(y) \tag{42}$$

where H_{00} is a mean constant depth of the fluid. The $H_b(y)$ is related to the zonally averaged mean zonal wind $u_b(y)$ geostrophically; $u_b(y)$ is given by

$$u_b(y) = L - M\cos\{\pi(y) - y_0)/Na\} \tag{43}$$

where L, M and N are specified constants and a is the planetary radius.

In our simple atmosphere, processes that would normally maintain the basic zonally symmetric flow, such as a very slowly varying radiational heating gradient, cannot be included. Thus, in order to maintain the symmetric "climate" of the model, we assume that the zonal wind relaxes back towards the basic state. This relaxation is accomplished by using a Rayleigh friction formulation with a damping rate b; (29) would then take the form

$$u_t - fv + I(u) = -gmH_x - \alpha u + \Delta b\bar{u} \tag{44}$$

where Δ is a Dirac delta function, defined such that the relaxation function is zero except for the zonally symmetric part of the flow.

To introduce a longitudinal variation into the basic flow, we specify a particular form to the mass source–sink system M in (31). The form we choose matches the stationary Kelvin wavelike structure which is consistent with both the observations and theory for quasi-stationary flow at low latitudes as defined by Webster (1972) and Gill (1980); i.e., we let

$$M = M_b(x, y) + M'(x, y, t) \tag{45}$$

where M_b is the mass source–sink function that generates the equatorial basic shear and M' is the transient forcing function to be defined later. The form M_b is given as

$$M_b = \kappa \exp\{-y^2/y_1\} \cdot \cos(sx) \tag{46}$$

where κ is a specified constant and y_1 so chosen to provide a 1000 km e-folding scale about the equator.

d. Generation of transient forcing functions

By a suitable definition of M' in (46), it is possible to impose forcing of arbitrary form, scale and amplitude anywhere on the sphere. In our study, transient forcing functions of the form

$$M' = EJ(x, y)\,\tau(t) \tag{47}$$

where E is an amplitude function ($=5 \times 10^{-3}$) and the spatial and temporal functions, $\kappa(x, y)$ and $\tau(t)$, are defined as

$$J(x) = \exp(-|x - x_0|/2)\exp(-|y - y_0|^2/4) \tag{48}$$

$$\tau(t) = (t^3/(2\delta^3))\exp(-t/\delta). \tag{49}$$

The spatial function follows the form of WH and the temporal function the "fast" form of Lim and Chang (1983). Figure 11 shows $\kappa(x)$ (upper panel) and $\tau(t)$ (lower panel) where the constants x_0, y_0 and δ are defined to place the forcing functions at an arbitrary location (x_0, y_0) and provide a 2-day e-folding time scale.

5. The nonlinear basic states

In all integrations, a spherical domain confined between ±60° of latitude was chosen. Three basic states were used: namely, a state at rest and two nonlinear balanced basic states which contain both stretching and shearing deformation. These are meant to match the extremes of the observed horizontal variation shown in Fig. 4. The three states will be referred to as the Z (basic state at rest), the WW ("weak" westerly) and the SW ("strong" westerly) basic fields, respectively.

To generate the WW and SW basic states, the fully nonlinear model (29)–(31) and (32)–(34), together with the forcing function definitions (45)–(46), was integrated for 100 days with the H_{00} of (42) set at 2000 m for consistency with the analytic results and the ex-

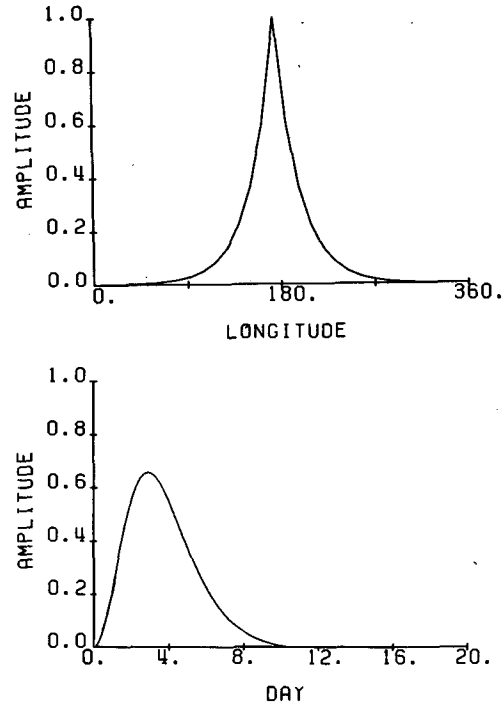

FIG. 11. The spatial [$J(x)$, upper diagram] and temporal [$\tau(t)$, lower diagram] forms of the forcing function of (48) and (49).

periments of WH. As the forcing functions are constant with time, the model reaches an equilibrium rather rapidly. Rayleigh friction with a 20-day e-folding decay rate was used. Figure 12 shows the resultant equilibrium velocity fields in vector format with the height field (dashed lines) superimposed. The heavy solid line encloses the regions of easterlies. Although simpler than the field shown in Fig. 2, the simulated basic fields possess the elements and magnitudes of the observed fields, including both shearing and stretching deformation. Purposely, the fields are quite similar to those generated by WH.

Prior to forcing the three basic fields, their barotropic stability was tested. In all cases, the fields satisfied the positive $(\beta - \bar{u}_{yy})$ criterion. Furthermore, more exotic hydrodynamical instabilities that may be associated with the shear and stretch combinations were tested implicitly by WH. They found that the response within the WW and SW basic states depended *solely* on the location of their extratropical wave sources. Clearly, this result suggests that the dispersion of waves is through a hydrodynamically stable basic state. A hydrodynamically unstable basic state would be unstable to any perturbation, irrespective of location. We will show further tests of the stability of the basic fields in section 8c.

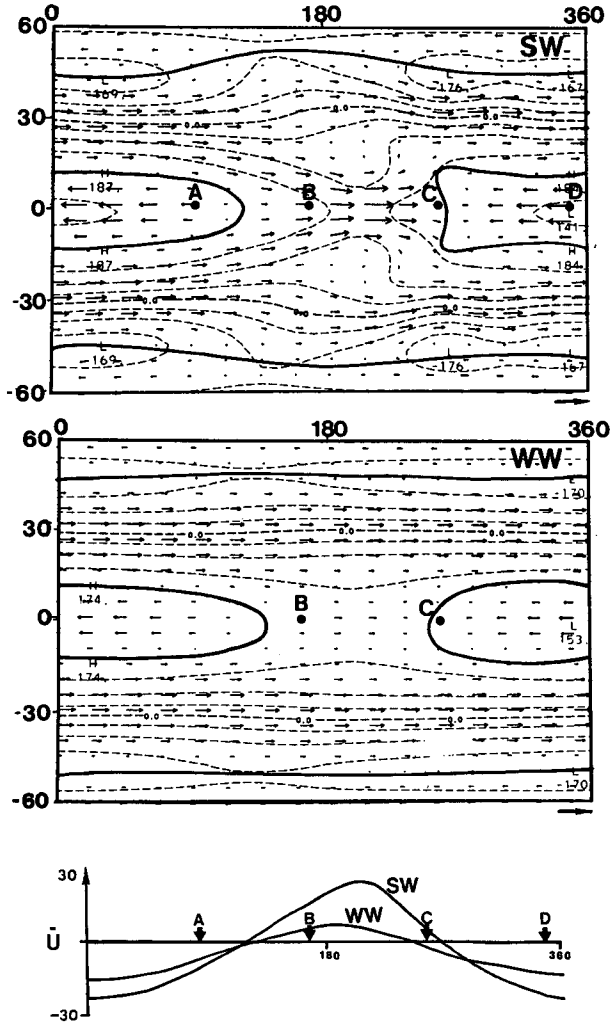

FIG. 12. Longitude–latitude plot of the velocity vectors and height fields of the nonlinear basic fields of (a), the strong westerly (SW), (b), the weak westerly states (WW), and (c) the zonal wind speed profile along the equator for the WW and SW states indicating the locations of the initial forcing.

6. The numerical experiments

The Z, WW and SW basic fields act as the initial conditions for the linear numerical experiments. Using a basic state $\bar{u}(x, y)$, $\bar{v}(x, y)$ and $\bar{h}(x, y)$, defined in (21), and calculated by the nonlinear model (see Fig. 12), the linear model [(29)–(31) with (39)–(41)] was integrated for 25-day periods relative to the perturbation functions (47)–(49) located at a number of longitudes. Relative to the coordinates of Fig. 12, the forcing functions were located along the equator at longitudes 80°, 170°, 260° and 350° which have been denoted by the letters A, B, C and D for easy recognition. The black dots on Fig. 12 indicate the central locations of the function (48). Figure 12c shows the amplitude of the basic flow along the equator for both the WW and SW states and also indicates the positions of the forcing for each of the experiments.

7. Results of the numerical experiments

a. Perturbation of the zero basic state (Z)

Figure 13 shows a longitude–time section along the equator of the perturbation zonal velocity component (u') for the 25-day period of the experiment. The corresponding nonlinear basic zonal wind field along the equator (in this case zero) is shown along the top of each section. The location of the forcing, given by the expressions (48) and (49), is indicated by the arrow along the abscissa.

The response within the zero basic state is extremely simple. After the initial forcing (placed at 170°, position B) diminishes, the predominant mode appears as a westward propagating Rossby wave. The mode merely propagates westward and undergoes a steady dissipation in time. Clearly, the form of the response is independent of the location of the forcing.

b. Perturbations of the weak westerly basic state (WW)

Longitude–time sections of the perturbation fields generated by forcing located at 170° (B) and 260° (C) of longitude are shown in Fig. 14a, b. An arrow identifies the central location of the initial forcing defined by (48) and (49). Initially, the response of the two cases are very different to one another. At this stage, strong perturbations exist in the vicinity of the forcing. As the forcing function diminishes (see Fig. 11), westward propagation occurs, although in a slightly more com-

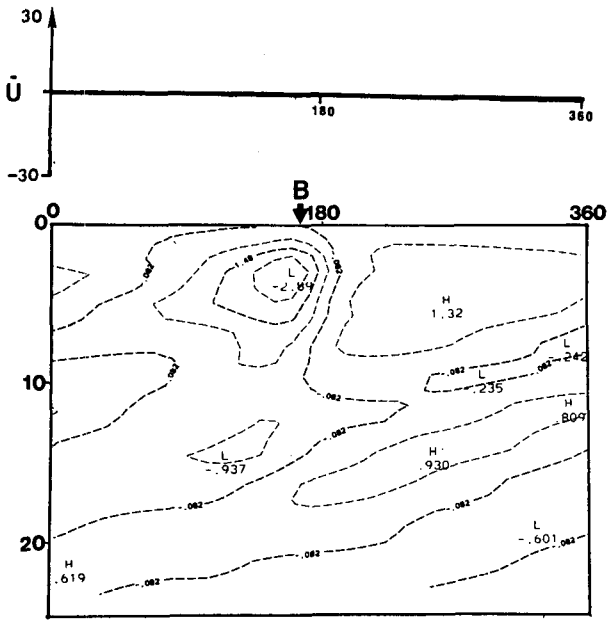

FIG. 13. Longitude–time section of the perturbation velocity component for the first 25 days along the equator of the experiment with a basic state at rest. The upper panel shows the mean zonal wind component of the basic state along the equator. The location of the initial forcing is indicated by B.

plicated manner than with the Z basic state. In the region of the weak equatorial westerlies, there is a slower westward propagation. We can examine this behavior in the vicinity of the westerlies more clearly by constructing longitude–time plots (Fig. 15a, b) of h'^2 which is proportional to the wave energy density, ϵ, of (26). After a period of time, the wave energy flux on the eastern side of the equatorial westerly maximum is about 30%–50% higher than elsewhere along the equator.

Figure 16 shows the perturbation height and velocity fields as a function of longitude–latitude after 25 days of integration. Very large scale perturbations can be seen in midlatitudes which are in addition to the relatively large zonal velocity component near the equatorial westerlies. This latter point is illustrated with a similar plot shown in Fig. 17 of the perturbation relative vorticity (ζ). Relatively strong centers of ζ exist on either side of the equator in the vicinity and to the east of the equatorial westerly maximum. These solutions are consistent with the simpler WKBJ calculations where we found that weak longitudinal stretch of similar magnitude was sufficient to create a wave energy saturation region.

The westerlies appear to be the emanation region for relatively weak wave trains propagating into the Northern and Southern Hemispheres. We will discuss and test this observation in section 7d.

c. *Perturbation of the strong westerly basic state (SW)*

Figure 18a–d shows a longitude–time section of u' along the equator for a 25-day period for the four locations of forcing (A–D) indicated in Fig. 12 within the SW basic state. Once again, early in the integration the perturbation flow field is large only near the location of forcing. However, with time, the perturbation moves and concentrates to the region east of the westerly maximum. All cases show a maximum response in the region between 200° and 250° after a period of time. Figures 19a–d show the same longitude–time sections but for h'^2. The maxima in the regions of negative longitudinal stretch indicates a distinctive regional accumulation of wave energy. Accompanying the accumulation is a shortening of the longitudinal scale and a lengthening of the period of modes. Both features are consistent with the simple analysis presented earlier in section 3.

The horizontal plots of the velocity fields and the relative vorticity are shown in Figs. 20a–d and 21a–d, respectively. Similar in some respects to the response

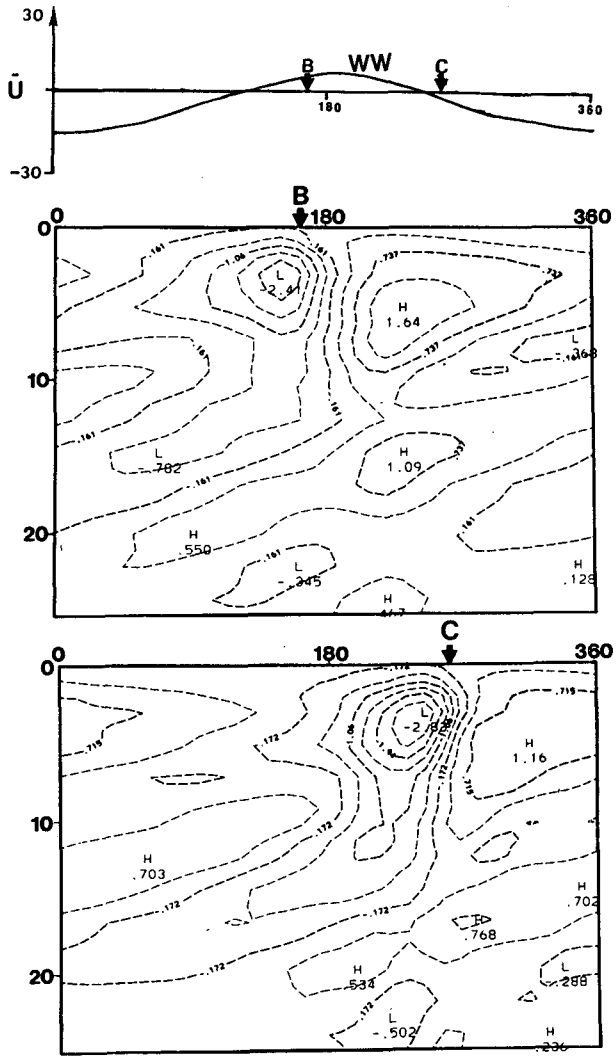

FIG. 14. As in Fig. 13 but with the weak westerly basic state (WW). Forcing is located at B, within the equatorial westerlies, (upper panel) and at C, near $\bar{u} = 0$ (lower panel).

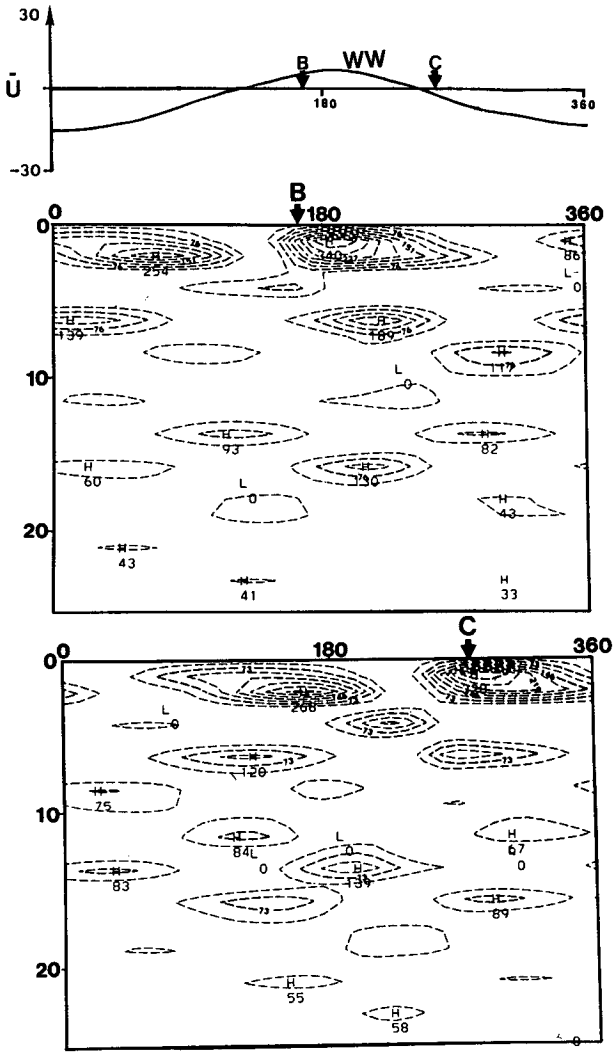

FIG. 15. As in Fig. 13 but for h'^2 field in the WW basic state. Forcing is located at B (upper panel) and C (lower panel). The quantity h'^2 is proportional to the wave energy density.

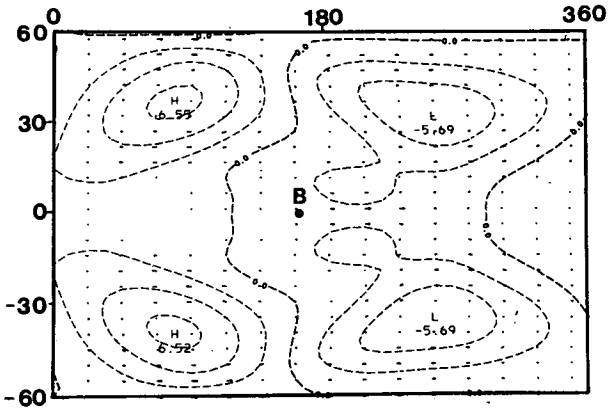

FIG. 16. Longitude–latitude section of the perturbation velocity and height field after 25 days of integration for the WW basic state. The $\bar{u}$ = 0 isopleth from Fig. 12 is shown to demark the easterlies and westerlies. Note the maximum perturbation in the vicinity of the mean equatorial westerlies. The central location of the forcing (equator, 170° longitude) is indicated by a black dot and the letter B.

with the WW basic state, the perturbations fields show clear evidence of local perturbations along the equator. Although the details of each experiment are different, we can see, with reference to Fig. 12, that the scale of the motion in the region of accumulation is relatively small. The perturbation scale change along the equator is also apparent from the longitude–time sections (i.e., Figs. 18 and 19).

Finally, it is worth pointing out once again that the region of energy accumulation to the east of the equatorial westerly maximum appears to be the emanation region for extratropical wave trains.

d. Localized wave train emanation regions

Local emanation regions of wave trains from the equatorial regions to the extratropics were noted for both WW and SW exponents. To substantiate their existence, we plot time–longitude sections of u' along 30°N for the four SW cases in Fig. 22a–d. The lettering A, B, C and D refer to the longitude where the initial forcing was applied at the equator as shown in Fig. 12c.

The details of the four sections are quite different, although there are a number of very important common features. The perturbation develops a substantial magnitude only after 10 days or so. From Fig. 11, we note this is 5 days *after* the equatorial forcing function reaches its maximum value so that the response structure *follows* the time at which the amplitude in the accumulation region along the equator reaches a maximum. But, most importantly, this sequence of events takes place in the same longitude belt (between 180° and 270°) in each case. That is, the amplification at 30°N after day 10 is taking place immediately poleward of the equatorial accumulation region identified earlier. Together, the timing and location of the response at 30°N adds credence to the concept of a localized low

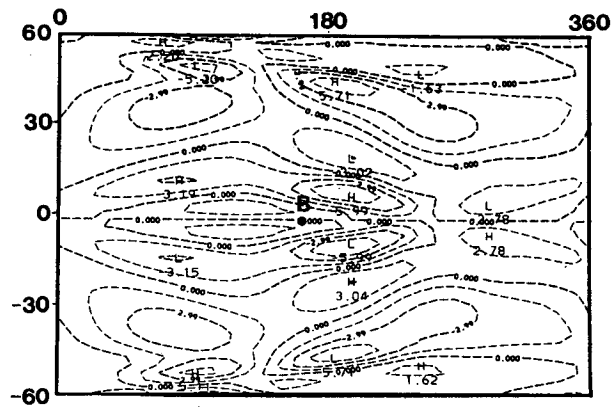

FIG. 17. As in Fig. 16 but for the perturbation relative vorticity field within the WW basic field.

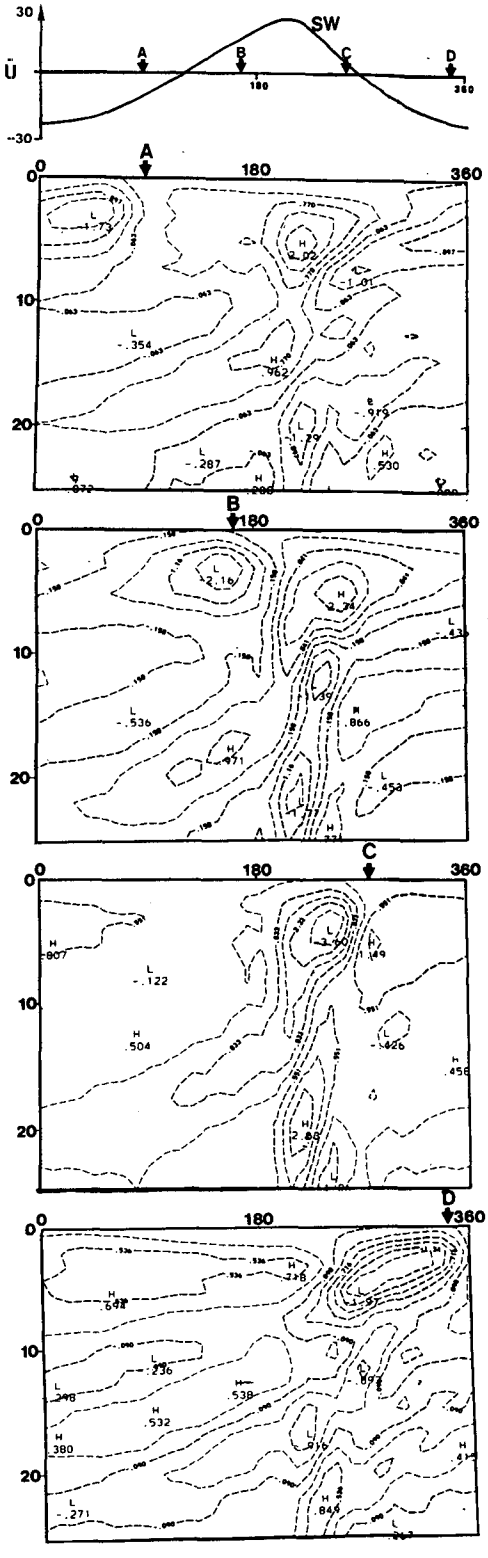

FIG. 18. Longitude–time section as in Fig. 13 except for the u' field produced by forcing located at A, B, C and D as indicated in Fig. 12a along the equator for the strong westerly basic state (SW).

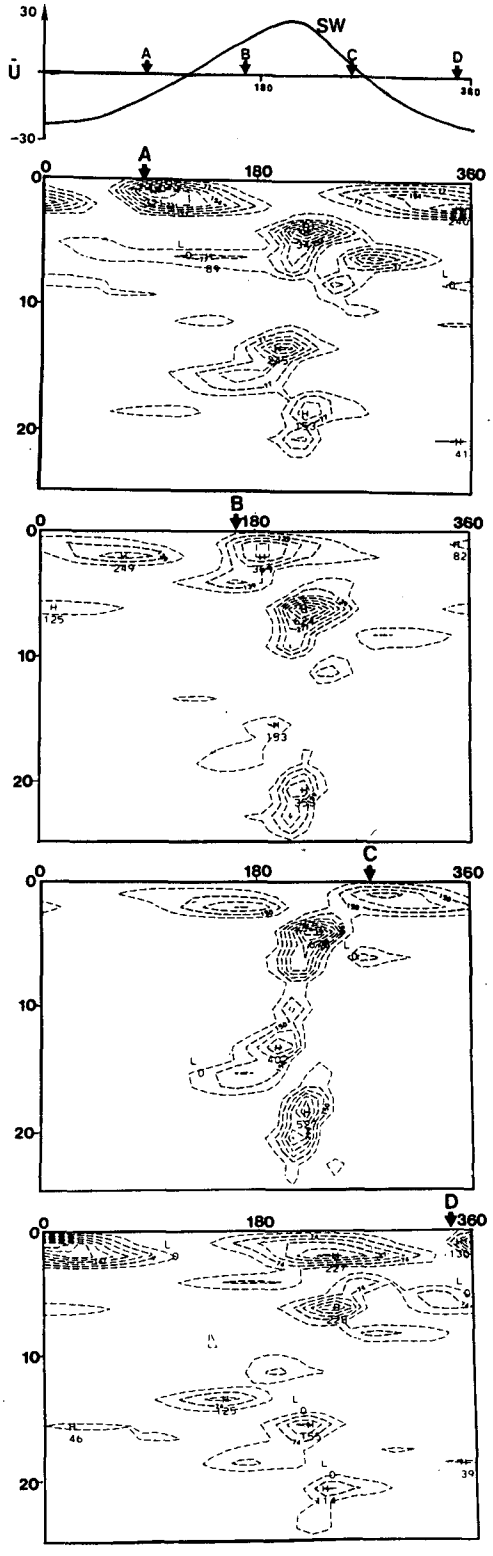

FIG. 19. Longitude–time section as in Fig. 13 except for the h'^2 field produced by forcing at A, B, C and D for the strong westerly basic state (SW).

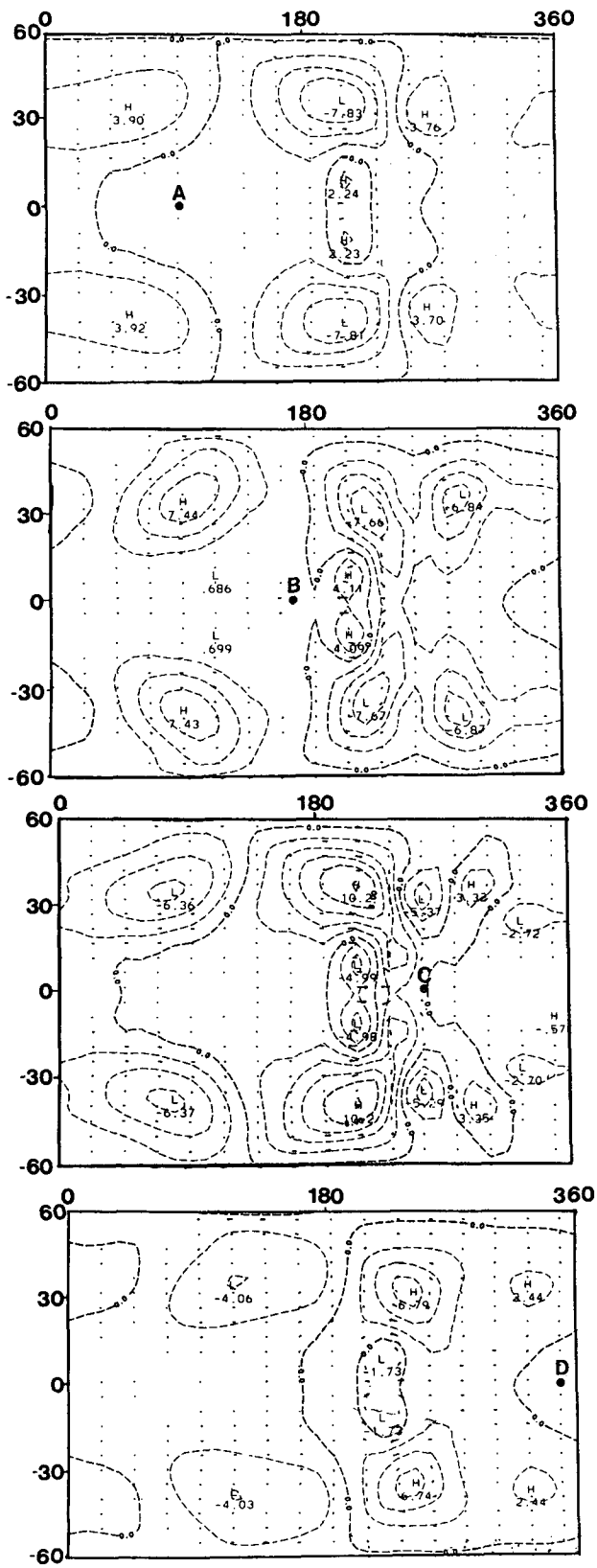

FIG. 20. Latitude–longitude plot as in Fig. 16 except for the perturbation velocity and height fields produced by forcing located at A, B, C and D for the strong westerly basic state (SW) after 25 days of integration.

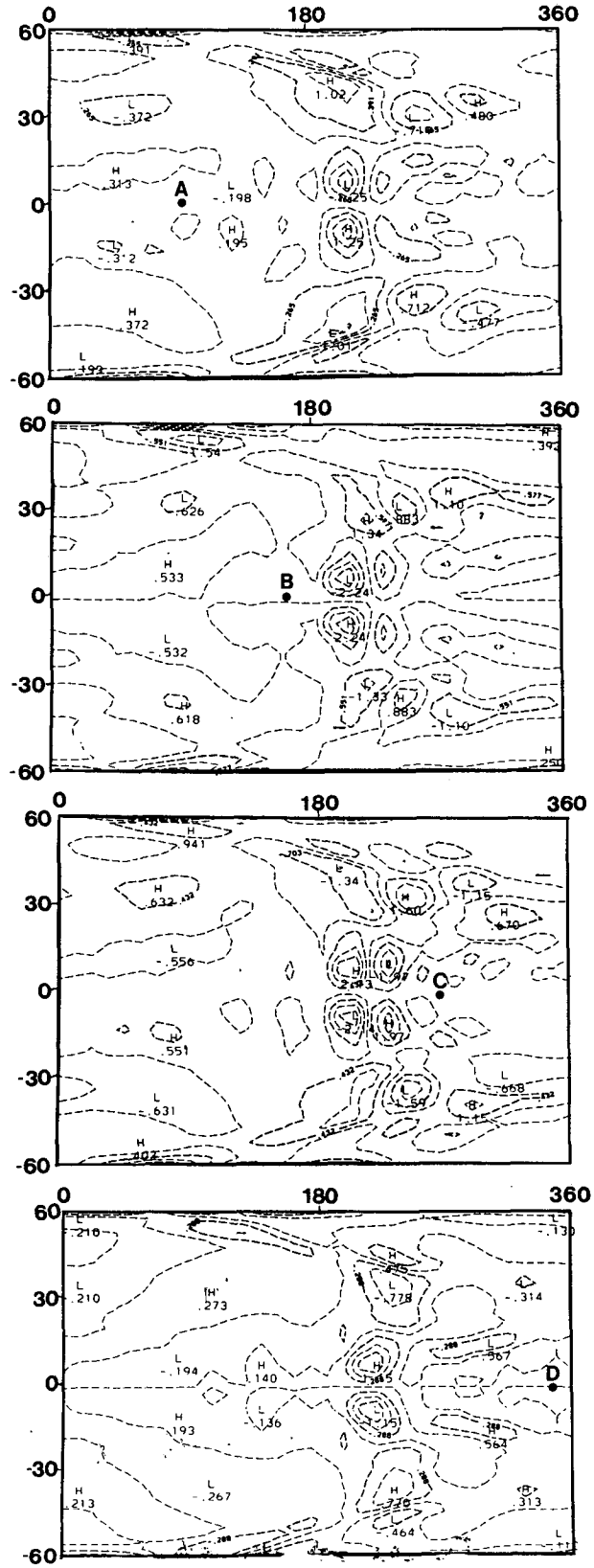

FIG. 21. As in Fig. 16 except for the perturbation relative vorticity field produced by forcing located at A, B, C and D after 25 days of integration.

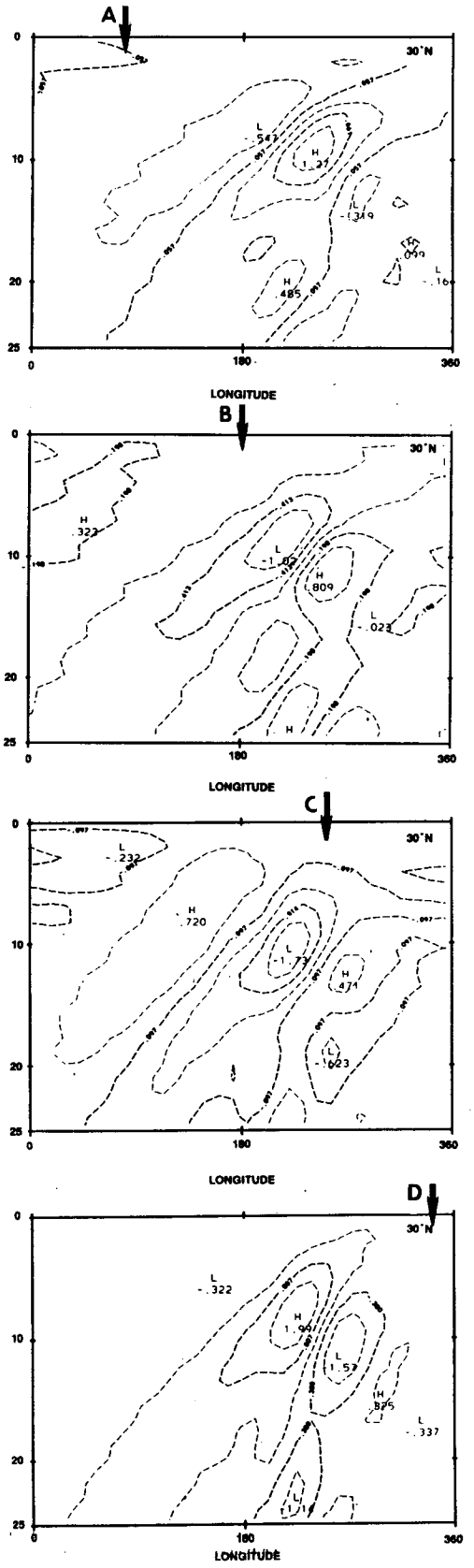

latitude wave train emanation region. A series of longitude–latitude plots through the period of integration show clearly the same sequence and timing of the middle latitude response as in Fig. 22, although symmetrically about the equator. This sequence is not shown for reasons of brevity. The change in the form of the response from the region of forcing to the region of accumulation, where it becomes a laterally propagating mode is puzzling. We address this point in section 8b.

8. Summary, speculations and extensions

a. Motivation

The initial impetus for the study stems from a need to reexamine the mechanisms that produce the transient variance maxima in the vicinity of the equatorial westerlies in the upper troposphere of the Pacific and Atlantic oceans. Earlier, WH have shown that it was possible to produce the regional $\overline{PKE}$ maxima by propagation of waves from the extratropics through the equatorial westerlies via the "westerly duct." Although the physical foundation of the WH study still appears sound, it left open the possibility that there were other, additional, energy sources that may be responsible for the regional energy accumulation.

It had been noted by WH and Arkin and Webster (1985) that the $\overline{PKE}$ maxima did not coincide spatially with the convective maxima along the equator. In fact, Fig. 2, which summarizes Arkin and Webster's results, shows that they are completely out-of-phase in longitude. Thus the transient energy sources, if they were to exist within the equatorial regions, had to be remote sources. For this to occur, there are three criteria that must be satisfied: 1) that there are transient energy sources within the tropics; 2) that the ability exists for the efficient transfer of the energy from one region of the tropics to another; and that there are mechanisms which allow the energy to be accumulated in the regions of the westerlies.

Mechanisms necessary to satisfy the first two criteria are identified readily. Organized regional convective activity acts as the energy source and the equatorial-trapped modes possess phase and group characteristics that allow for an efficient transfer of energy along the equator. However, the search for a mechanism to satisfy the third criterion is more elusive. To account for the regional longitudinal energy trapping, it was hypothesized that the longitudinal stretching deformation of the basic flow of the tropics so alters the characteristics of the equatorially trapped modes that their Doppler shifted group speed becomes locally zero, producing a

FIG. 22. Time–longitude of perturbation zonal velocity component plots along 30°N for the SW basic state. The letters above the four panels indicate the location of the forcing along the equator as shown in Fig. 12a.

local convergence of energy to the east of the equatorial westerlies.

b. *Testing of the hypothesis*

The hypothesis based on an assumption of the importance of mode characteristic modification by the longitudinal stretch of the basic flow was tested using two surrogate fluid systems. The first was the rather restrictive analytic system. The second was a numerical model of a free surface barotropic system containing a basic state which contained both shearing and stretching deformation. Both systems were capable of possessing divergent barotropic modes.

1) THE ANALYTIC RESULTS

To help define an appropriate analysis system with which to test the hypothesis, the difference between barotropic and divergent barotropic modes at low latitudes was discussed. Barotropic modes possessed both zonal and meridional group and phase speeds. On the other hand, equatorial divergent modes were characterized by an absence of meridional components and possessed only zonal group and phase speeds; i.e., they were equatorially trapped. Noting the divergent nature of equatorial transients, the equatorially-trapped modes were emphasized.

Within approximations that allow analytic tractability (specifically that the basic flow is time independent and *locally* constant), it was shown that for realistic values of longitudinal stretch zeros exist in the local Doppler shifted group speed of the equatorially trapped Rossby waves. Given that the basic state considered was time-independent, such that the modal Doppler-shifted frequency is constrained to remain constant along a ray, it was shown that in regions of negative stretch (i.e., $\partial\bar{u}/\partial x < 0$) that the scale of the modes must shorten, whereas in regions of positive stretch (i.e., $\partial\bar{u}/\partial x > 0$) the longitudinal scale must lengthen. The consequences of this scale change is to alter the group characteristics of the mode (see Fig. 7) and produce a convergence of wave energy density in regions of negative stretch and a divergence in regions of positive stretch. In the simple trigonmetric basic state used in the analytic calculations, a maximum energy accumulation occurs where

$$\frac{\partial\bar{u}}{\partial x} < 0\,|_{\max}.$$

That is, the maximum accumulation occurs on the eastern side of the westerly maximum.

Figure 23 summarizes schematically the propagation through a basic flow $\bar{u}(x)$ of three equatorially trapped modes forced near A, B and C whose group speeds are in the same range as the observed zonal wind along the equator. It was noted in Fig. 6a, b that this similarity

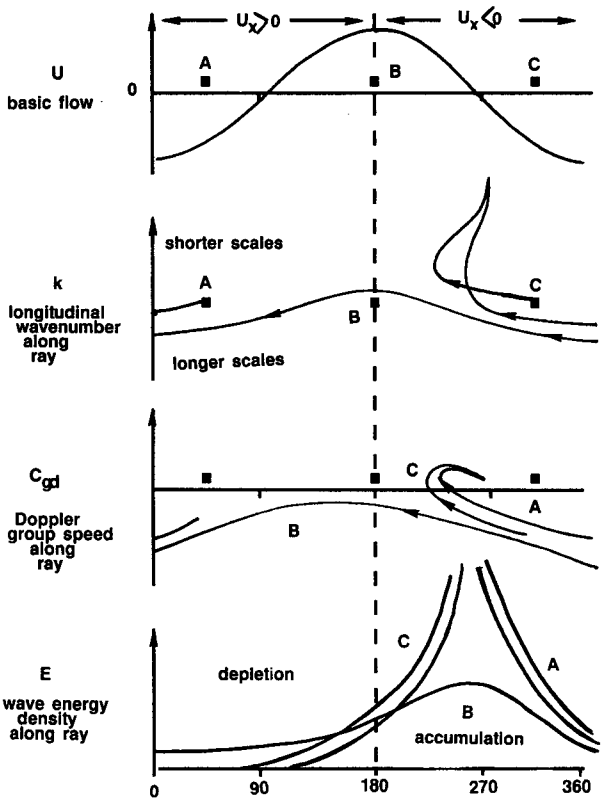

FIG. 23. Schematic diagram representing the results of the WKBJ analysis for equatorially trapped Rossby waves moving through a basic state with longitudinal stretch as shown in the upper panel. Wave sources are located at A, B and C along the equator. Second panel shows the variation of the wavenumber along the three rays as given by (23). The third panel shows the variation of the Doppler-shifted group speed along the ray according to (19). A and C are longitudinally trapped whereas B, the exceptional mode which always possess a $C_{gd} < 0$, is free to propagate around the equator. The bottom panel shows the wave energy density variation along the rays from (24). Regions of energy depletion and accumulation along the equator are indicated.

of $\bar{u}$ and C_g occurs for realistic scales and equivalent depths. The schematic is divided into four panels representing, respectively, the zonal wind along the equator (upper panel), the longitudinal wavenumber along a ray [second panel, k from (23)], the longitudinal group speed along a ray [third panel, C_g from (19)] and the wave energy density [bottom panel, ϵ from (25)] along a ray. The $\bar{u}$ distribution, as shown, possesses negative stretch between 180° and 360° and positive stretch between 0° and 180°. The schematic shows two modes, A and C, whose initial location and scales allow longitudinal trapping where $\bar{u} = 0$ which, in this case is where

$$\frac{\partial\bar{u}}{\partial x} < 0\,|_{\max}$$

occurs. The schematic also shows the exceptional mode *B* discussed in detail in section 3c. Such a mode must

possess a group speed such that $C_{gd} < 0$ at all points around the equator which, for a given basic state, occurs only for the largest scales of motion along the equator.

In summary, despite the limitation of the WKBJ approximations, the analysis of the simple system provided a physical basis for the development of a more complicated model. In particular, it provided physical mechanisms, determined a priori, to be tested in the more complete system.

2) THE NUMERICAL RESULTS

To reduce the uncertainties arising from the scale constraints of the WKBJ approximations, experiments were performed using a less restrictive free surface barotropic model. Here, waves were excited within a fully nonlinear two-dimensional basic state containing both shearing and stretching deformation which was generated using a nonlinear model. Within this system, too, waves provided energy accumulation in the same region of the tropics, irrespective of the location of the forcing. As before, accumulation of energy occurred where $\partial\bar{u}/\partial x < 0$. However, the model's greater degrees of freedom helped isolate a new property and one that may be of fundamental importance to the physics of communication between low and high latitudes. Experimental results showed that the region of wave energy accumulation (i.e., the regions of negative stretch) was also the region of wave train emanation to the extratropics. These results were reinforced by studying extratropical time–longitude sections. In other words, *regardless of the longitude of the equatorial forcing, waves emanated from the same tropical region; the region immediately to the east of the equatorial westerlies, towards the extratropics.*

One of the puzzling aspects of the numerical model is the manner in which the apparently trapped modes in the vicinity of the accumulation point adopt a laterally propagating character. The WKBJ theory (see section 3) does not help us understand such a mode transition, but only the mechanism that creates the accumulation region itself. It is quite possible that the emanation phenomena is merely a transition of the character of the modes as they propagate along the equator from source regions within the easterlies, where they are severely trapped about the equator and laterally evanescent, to the region of westerlies where the accumulation regions exists and where the modes can become latitudinally propagating (Lim and Chang, 1983). With this explanation in mind, it would seem that there are two criteria which choose where the emanation of higher latitudes will occur. The location is chosen by where the accumulation zone exists along the equator and by the ability of the modes in the region to propagate laterally within the environment. If the accumulation zone were to reside in a different wind regime (e.g., somewhere in the equatorial easterlies) emanation to higher latitudes may not occur or may be much weaker. A fuller explanation of the emanation character of the modes may require the more extensive analysis described in section 8d.

Another interesting feature of the numerical results portrayed in longitude–time sections is the fairly regular amplitude growth or pulse about every 10 days that is superimposed on the general amplitude decay following excitation in the accumulation zone. A careful examination of Fig. 18 shows the amplitude increase corresponds to the propagation of a large-scale mode through the accumulation zone from east to west. Presumably, the propagating wave is the grave untrapped mode discussed in section 3e.

Throughout the text it has been suggested that the accumulation phenomena occur over a wide range of H_0. In fact, the WKBJ analysis showed longitudinal trapping for an equivalent depth of 100 m. Figure 24 shows that both the accumulation *and* the emanation phenomena are also apparent for smaller H_0 in the numerical model. The upper panel shows a "strong westerly" basic state, derived in the manner described in section 5, for H_0 = 500 m. The lower panel shows the longitude–latitude distribution of perturbation

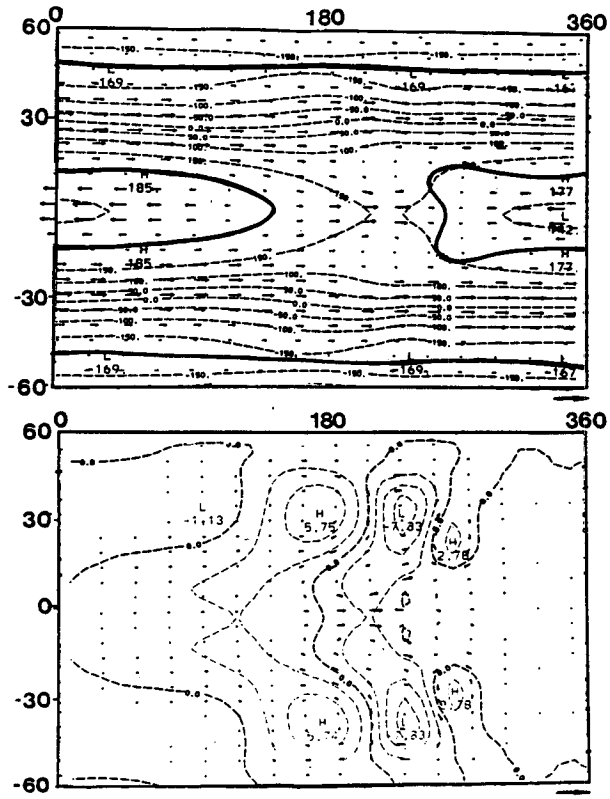

FIG. 24. Latitude–longitude plots of (a) a "strong westerly" basic state with H = 500 m, and, (b) the perturbation velocity and height field 25 days after transient forcing at point D in Fig. 12.

height and velocity at 25 days following a transient forcing at point D. The response should be compared with Fig. 20 where many similar features are apparent.

c. *Alternative explanations*

It is important and necessary to review and, if possible, reject other candidate physical mechanisms that may explain the apparent wave energy accumulation and emanation phenomena. Particularly, it is necessary to question whether the regional energy accumulation may be a result of some form of hydrodynamic instability.

To investigate an instability hypothesis with full rigor requires an eigenvalue–eigenvector analysis of the basic states used in the study. An exhaustive eigenanalysis of a particular two-dimensional equatorial basic flow (specifically, the 300 mb climatology of the NCAR Community Climate Model) has been undertaken by Branstator (1985). But this analysis is of a purely barotropic system, and thus only of the rotational part of the climatology, and not the more pertinent divergent system studied here. The eigenanalysis of a free surface barotropic system is considerably more difficult than Branstator's analysis and beyond the scope of this study. However, it is possible to list the substantial reasons why we expect that hydrodynamical instability to be a relatively poor candidate to explain the results of the numerical model. These are:

(i) The WKBJ analysis of the behavior of the appropriate equatorial modes in a flow with longitudinal variation has provided an a priori expectation of the location of the wave energy accumulation regions along the equator and the characteristics of the waves in this region which was validated in the numerical experiments. The physical explanations involve only wave dynamics and not stability arguments.

(ii) In terms of simple shearing barotropic instability, the basic fields WW and SW, as described in section 5, are stable. At all locations within the domain, $(\beta - u_{yy}) > 0$.

(iii) The WH integration using the WW and SW states suggest a robust stability of the WW and SW basic fields. Webster and Holton show that the response of the basic fields at low latitudes and the extratropics were functions only of the *location* of the extratropical forcing relative to the two-dimensional basic state. If the basic states were unstable, the instability would grow irrespective of the location of the forcing. As one further test of this stability, the strong westerly basic state (Fig. 12a) was randomly perturbed at all points. The maximum amplitude was chosen to be ± 3 m s^{-1}. With the perturbed initial state the model was integrated for 50 days. Figure 25 shows perturbation kinetic energy (PKE), the perturbation available potential energy (APE) and the total perturbation energy (APE + PKE), integrated over the entire model domain. The stability of the strong westerly basic state is demonstrated by the decay of the response with time.

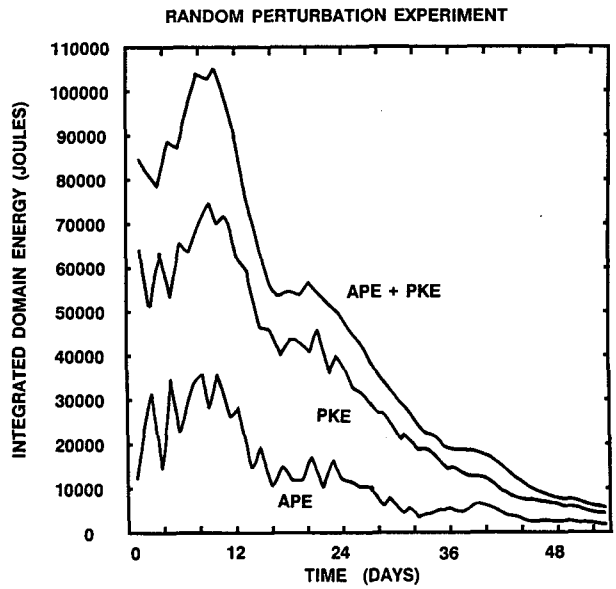

FIG. 25. Evolution of the perturbation kinetic energy (PKE), available potential energy (APE) and the total energy (APE + PKE) summed over the entire model domain following a random perturbation (maximum perturbation $\pm$ m s^{-1}) of the strong westerly basic state of Fig. 12a.

In summary, it would appear that (i) through (iii) demonstrate that hydrodynamical instability is not relevant in the explanation of the phenomena discussed here.

d. *Speculations*

Results from the two independent models developed in this study have shown a consistent behavior in producing concentrations of PKE in the region equatorial westerlies that match the observed locations. There are, however, results from other, independent, studies that may also be consistent with the concept of wave energy accumulation regions and wave train emanation zones. Although these results are reported more fully elsewhere, they are described briefly below to indicate that the concepts developed in the study may be more general.

O'Lenic et al. (1985) studied the impact of a poorly defined tropical data base on global weather prediction with the NMC global spectral model.

Two major results are of particular relevance here. First, after a few days, the tropical atmosphere showed a fairly similar distribution of perturbations within the tropics irrespective of where it was forced. Second, regardless of the location of the forcing within the tropics, the response at higher latitudes is very similar; i.e., the response in the extratropics appears to be phase-locked.

Quite possibly the propagation of difference anomalies out of the tropics is following a routing decreed by the wave-energy accumulation region–emanation mechanism.

In another study, Geisler et al., (1985) investigated the sensitivity of the response of the NCAR-CCM (the National Center for Atmospheric Research Community Climate Model) to the positioning of a sea surface temperature anomaly as it was moved progressively eastward of the dateline. Although the positions of the perturbations varied over a smaller longitudinal range than the NMC experiments or the simpler model experiments, described above, they found after 90-day simulations that the response in midlatitudes was essentially the same irrespective of the position of the tropical sea surface temperature anomaly. Specifically, Geisler et al. found that the extratropical response to all experiments was the geographically fixed PNA (Pacific–North America) pattern described observationally by Horel and Wallace (1981), and many others. Although the magnitude of the features changed somewhat, the midlatitude response was phase-locked.

Geisler et al. noted that the CCM insensitivity to the longitudinal anomalous heating location was in agreement with the conclusions of Simmons et al. (1983) who interpreted a persistent extratropical response in a simpler model as the fastest growing barotropically unstable mode in midlatitudes. However, we must ask whether or not we can interpret the results through the same combination of the wave energy accumulation regions and wave emanation zones of the tropical atmosphere developed in this study. It might be added that the eigenanalysis of Branstator (1985) suggests that something beyond the Simmons et al. theory is needed to explain fully the phase locking of the Geisler et al. results.

A further phenomena which may be of relevance here is the character of the middle-latitude response to the low-latitude 40–60 day mode, first described by Madden and Julian (1972). Subsequent studies (particularly, Weikman et al., 1985, Lorenc, 1984) have refined its definition with careful diagnostic studies. Over the period of its oscillation, the mode is seen to be highly convective in the regions of warm sea surface temperature from the east Indian Ocean to the central Pacific Ocean. During this time, the convection moves through the climatological convective maximum (e.g., see Fig. 2) in phase with the 40–60 day mode. Lau and Phillips (1986) have shown, using principal component analysis, that the propagating convection associated with the 40–60 day mode possesses a distinct midlatitude response. However, irrespective of the phase of the tropical forcing, Lau and Phillips found that the response in the midlatitudes was phase locked.

In summary, both the NMC global spectral and the NCAR CCM models may be showing responses to perturbations that are consistent with the linear analytic model and the free-surface barotropic model presented in this paper; i.e., the longitudinal basic state of the equatorial regions may determine where the energy of the perturbation will propagate and accumulate. The very similar response at high latitudes to vastly different equatorial forcing suggests that the energy may emanate from the same region in the tropics. Furthermore, the diagnostic study of Lau and Phillips (1986) probably adds some credence, from an observational perspective, to the existence of accumulation and emanation concepts.

Finally, in this list of speculations, it is appropriate to construct a model of equatorial to extratropical teleconnections suggested by the model results and which is consistent with the three studies discussed here. Figure 26 is an attempt at such a construction. It shows an *equatorial teleconnection* by the equatorial longitudinally trapped modes between the regions of convection and negative longitudinal stretch (hatched areas) in the manner suggested in both analytic and numerical results. From the accumulation region, wave trains may be seen to emanate to higher latitudes in the manner of Hoskins and Karoly (1981) and Webster (1981, 1983). This emanation corresponds to the second stage of the mechanism; the *equatorial–extratropical wave-train teleconnection.*

There is a special significance to the concept of the tropical atmosphere possessing energy depletion and accumulation regions. It allows for a means of communication between remote parts of the tropical atmosphere or for an equatorial teleconnection; i.e., it provides a low latitude physical analogy to the tropical–extratropical Rossby wave-train teleconnection mechanism proposed by Hoskins and Karoly (1981) and Webster (1981). Because there appear distinct emanation regions from the tropics, the latter teleconnection mechanism also requires modification with the train origin anchored in the region of equatorial westerlies. In other words, the simple wave hypothesis existing between the anomalous heat source and the extratropics is replaced by two teleconnection patterns.

e. Extensions and further studies

There are a number of obvious extensions with respect to the modeling. The results presented in this paper were essentially linear even though relative to basic states generated by a nonlinear model. It appears essential that the investigation be extended into the fully nonlinear regime. Only then can the transition from the accumulation region along the equator to an emanation region to the extratropics be examined with some confidence.

It is important to examine the steady-state limit of the processes emphasized in this study. Geisler et al. (1985), for example, were concerned with time-mean anomalies of 1200-day general circulation model sim-

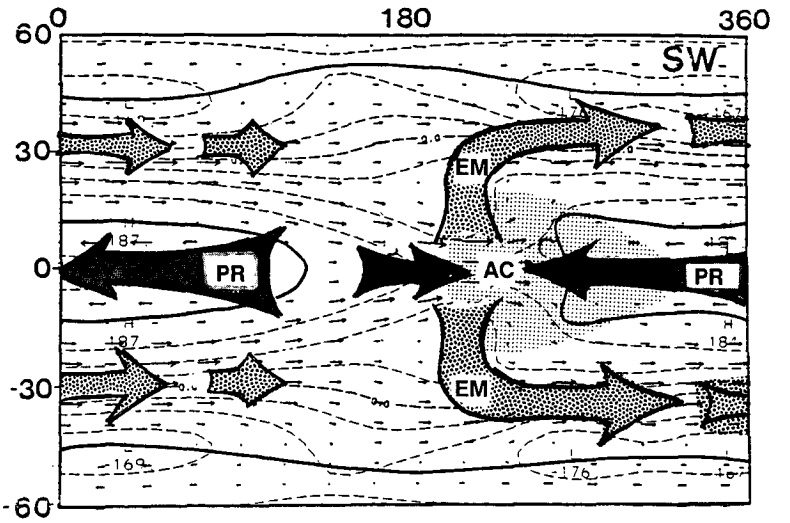

FIG. 26. Schematic diagram of the two stage teleconnection mechanism between the tropics and higher latitudes. The first stage, the equatorial teleconnection, shows wave energy propagation (PR) by the equatorially trapped modes (broad arrows) into regions of energy accumulation (AC) (shaded regions). The second stage, the tropical–extratropical wavetrain may be seen emanating to higher latitudes (EM) (broad arrows) from the equatorial accumulation regions.

ulations that we have attempted to interpret with the characteristics of transient modes. However, it is probable that there is a steady-state analogue. Time-mean steady-state equatorially trapped Kelvin waves possess both zero Doppler shifted phase and group longitudinal speeds owing to their dispersive nature. Equatorially trapped Rossby waves, on the other hand, are dispersive and have a nonzero group speed like their stationary extratropical counterparts. Consequently we may expect an anomalous remote response and energy accumulation influenced by the mean basic state in the very low frequency domain.

One of the major challenges that remains is the explanation of the mode transition between the region of easterlies and westerlies along the equator (see section 8b for discussion). To test whether or not the transition occurs as an evolution of the latitudinal modal structure of the equatorial modes as the modes propagate from an obstensibly easterly regime to the accumulation point within the westerlies, as might be suggested by Lim and Chang (1983), we are attempting to decompose the perturbation structure mode by mode. When this decomposition is achieved, merely following the individual modes in time will test the hypothesis.

Finally, an obvious extension of the study is to determine critically whether or not the mechanisms discussed in this paper are a mere hydrodynamical curiosity or possess some practical significance. The possibility that the energy accumulation–emanation mechanism may play a role in the atmospheric teleconnection is very appealing. But is there an application that may be relevant to extended global weather prediction? For example, can Fig. 10 be interpreted from a numerical weather prediction perspective? Given the paucity of data in certain tropical regions, can the concept of longitudinal trapping of some modes but the free propagation of others define a "region of influence" for the tropical atmosphere as Charney and Eliassen (1949) discussed for the long waves of the extratropics? Furthermore, are there oceanographic analogies to these concepts? For example, how do the oceanic equationally trapped modes which appear so critical in theory of El Niño, contend with a longitudinally varying oceanic basic state along the equator?

Acknowledgments. The authors would like to acknowledge J. R. Holton and G. Branstrator for stimulating discussions, our colleague J. M. Fritsch for interesting perspectives and the *Journal of Atmospheric Sciences* editing and review process, which introduced a number of improvements into the manuscript. We would also like to thank Mrs. Delores Corman and Mrs. Nancy Warner for typing the manuscript. This study was supported by the Atmospheric Sciences Division of the National Science Foundation under Grant ATM 83-18852. The National Center for Atmospheric Research provided computing facilities.

APPENDIX

Derivation of Equation (23)

Consider a flow that varies in space in a gradual manner such that the change over the wavelength of a mode is very small. Within this medium we can write

a simple expression between the absolute frequency ω_d (the frequency of oscillation occurring at a fixed point in space) and the relative frequency ω_r (the frequency of oscillation at a point moving with velocity v_i). Following Lighthill (1978), we can define the absolute frequency ω_d and the wavenumber k_i in terms of a phase function $\alpha(x_1, x_2, x_3, t)$ such that

$$\omega_d = \frac{\partial \alpha}{\partial t}, \quad k_i = \frac{\partial \alpha}{\partial x_i} \tag{A1}$$

Then, the relative frequency ω_r can be defined as

$$\omega_r = \omega_d - v_i k_i. \tag{A2}$$

In general form, a dispersion relationship for the mode can be written as

$$\omega_d = \omega_d(k_1, k_2, k_3, x_1, x_2, x_3) \tag{A3}$$

so that

$$\frac{\partial^2 \alpha}{\partial x \partial t} = -\frac{\partial \omega_d}{\partial k_i}\frac{\partial k_i}{\partial x_i} - \left.\frac{\partial \omega_d}{\partial x_i}\right|_{k_i} \tag{A4}$$

$$\frac{\partial k}{\partial t} + \frac{\partial \omega_d}{\partial k_i}\frac{\partial k_i}{\partial x_i} = -\left.\frac{\partial \omega_d}{\partial x_i}\right|_{k_i}. \tag{A5}$$

A dispersion relationship for an equatorially trapped Rossby wave may be written as (e.g., Gill, 1983):

$$\omega_r = -\frac{\beta k}{[k^2 + \beta(2n+1)/c]} \tag{A6}$$

so that if the mean flow is defined by $\bar{u}(x)$, we can obtain an expression for the absolute frequency from (A2) as

$$\omega_d = \bar{u}k + \omega_r = \bar{u}k - \frac{\beta k}{[k^2 + \beta(2n+1)/c]} \tag{A7}$$

Then between (A5) and (A7), we can obtain

$$\frac{\partial k}{\partial t} + \left(\bar{u} + \frac{\partial \omega_r}{\partial k}\right)\frac{\partial k}{\partial x} = -k\frac{d\bar{u}(x)}{dx}. \tag{A8}$$

If we define

$$\frac{dk}{dt} = \frac{\partial k}{\partial t} + \left(\bar{u} + \frac{\partial \omega_r}{\partial k}\right)\frac{\partial k}{\partial x} \tag{A9}$$

and noting that $[\bar{u} + (\partial\omega_r/\partial k)]$ is the Doppler shifted group speed C_{gd}, we obtain (23) between (A8) and (A9); i.e.,

$$\frac{dk}{dt} = \frac{\partial k}{\partial t} + \left(\bar{u} + \frac{\partial \omega_r}{\partial k}\right)\frac{\partial k}{\partial x} = -k\frac{d\bar{u}}{dx}. \tag{23}$$

Finally, we note that a very similar development exists for (25).

REFERENCES

Arkin, P., and P. J. Webster, 1985: Annual and interannual variability of the tropical-extratropical interaction: An empirical study. *Mon. Wea. Rev.*, **113,** 1510–1523.

Bjerknes, J., 1969: Atmospheric teleconnections from the equatorial Pacific. *Mon. Wea. Rev.*, **97,** 163–172.

Branstator, G., 1983: Horizontal energy propagation in a barotropic atmosphere with meridional and zonal structure. *J. Atmos. Sci.*, **40,** 1689–1708.

——, 1985: Analysis of general circulation model sea-surface temperature anomaly simulation using a linear model. Part I: Forced solutions. *J. Atmos. Sci.*, **42,** 2225–2254.

Bretherton, F. P., and C. J. R. Garrett, 1968: Wavetrain in inhomogeneous moving media. *Proc. Roy. Soc., London,* **A362,** 529–554.

Chang, C. P., 1977: Viscous internal gravity waves and low frequency oscillations in the tropics. *J. Atmos. Sci.*, **34,** 901–910.

Charney, J. G., 1969: A further note on the large scale motions in the tropics. *J. Atmos. Sci.*, **26,** 182–185.

——, and A. Eliassen, 1949: A numerical method for predicting the perturbations of the middle latitude westerlies. *Tellus,* **1,** 38–54.

Geisler, J. E., M. L. Blackmon, G. T. Bates and S. Munoz, 1985: Sensitivity of January climate response to the magnitude and position of equatorial Pacific sea surface temperature anomalies. *J. Atmos. Sci.*, **42,** 1037–1049.

Gill, A., 1980: Some simple solutions for heat-induced tropical circulations. *Quart. J. Roy. Met. Soc.*, **106,** 447–462.

——, 1982: *Atmosphere-Ocean Dynamics.* International Geophysics Series, Vol. 30, Academic Press, 662.

Hendon, H., 1986: Stream function and velocity potential representation of equatorially trapped waves. *J. Atmos. Sci.*, **43,** 3038–3042.

Holton, J. R., 1975: *The Dynamic Meteorology of the Stratosphere and the Mesosphere.* Meteor. Monogr., No. 37, Amer. Meteor. Soc., 216.

Horel, J. D., and J. M. Wallace, 1981: Planetary-scale atmospheric phenomena associated with the Southern Oscillation. *Mon. Wea. Rev.*, **109,** 813–829.

Hoskins, B. J., and D. Karoly, 1981: The steady linear response of a spherical atmosphere to thermal and orographic forcing. *J. Atmos. Sci.*, **38,** 1179–1196.

——, A. J. Simmons and D. G. Andrews, 1977: Energy dispersion in a barotropic atmosphere. *Quart. J. Roy. Meteor. Soc.*, **103,** 553–567.

Karoly, D., 1983: Rossby wave propagation in a barotropic atmosphere. *Dyn. Atmos. Oceans,* **7,** 111–125.

Keshavamurty, R. N., 1982: Response of the atmosphere to sea surface temperature anomalies over the equatorial Pacific and the teleconnections of the Southern Oscillation. *J. Atmos. Sci.*, **39,** 1241–1259.

Krishnamurti, T. N., 1971: Tropical east-west circulations during the northern hemisphere summer. *J. Atmos. Sci.*, **28,** 1342–1347.

Lau, K.-M., and H. Lim, 1984: On the dynamics of equatorial forcing of climate teleconnections. *J. Atmos. Sci.*, **41,** 616–176.

——, and T. J. Phillips, 1986: Coherent fluctuations of extratropical geophysical height and tropical convection in intraseasonal time scales. *J. Atmos. Sci.*, **43,** 1164–1181.

Lighthill, J., 1978: *Waves in Fluids,* Cambridge University Press, 504.

Longuet-Higgins, M. S., 1968: The eigenfunctions of Laplaces tidal equations. *Phil. Trans. R. Soc.*, **A262,** 511–607.

Lim, H., and C. P. Chang, 1983: Dynamics of teleconnections and Walker Circulations forced by equatorial heating. *J. Atmos. Sci.*, **40,** 1897–1915.

Lindzen, R., 1967: Planetary waves on a beta-plane. *Mon. Wea. Rev.*, **95,** 441–451.

Lorenc, A. C., 1984: The evolution of planetary-scale 200 mb divergent flow during the FGGE year. *Quart. J. Roy. Meteor. Soc.*, **110,** 427–442.

Madden, R., and P. Julian, 1972: Detection of a 40–60 day oscillation in the zonal wind in the tropical Pacific. *J. Atmos. Sci.*, **28,** 702–708.

Matsuno, T., 1966: Quasi-geostrophic motions in the equatorial area. *J. Meteor. Soc. Japan,* **44,** 25–42.

Murakami, T., and S. Unninayer, 1977: Atmospheric circulation during December 1970 through February 1971. *Mon. Wea. Rev.,* **105,** 1024–1038.

Mysak, L. A., 1980: Topographically forced waves. *Annual Reviews of Fluid Mechanics,* Vol. 12, Annual Reviews, 45–76.

O'Lenic, E., P. J. Webster and A. N. Samel, 1985: The effect of initial uncertainty in tropical analyses upon five-day forecasts with NMC's Global Spectral Model. NMC Tech. Note 311.

Opsteegh, J. D., and H. M. Van den Dool, 1980: Seasonal differences in the stationary response of a linearized primitive equation model: Prospects for long-range forecasting? *J. Atmos. Sci.,* **37,** 2169–2185.

Orzag, S., 1970: Transform method for the calculation of vector coupled sums: Application of the spectral form of the vorticity equation. *J. Atmos. Sci.,* **27,** 890–895.

Philander, S. G. H., 1986: El Niño y La Niña? *J. Atmos. Sci.,* **42,** 2652–2662.

Simmons, A. J., 1982: The forcing of stationary wave motion by tropical diabatic heating. *Quart. J. Roy. Meteor. Soc.,* **108,** 503–534.

——, J. M. Wallace and G. W. Branstator, 1983: Barotropic wave propagation and instability, and atmospheric teleconnection patterns. *J. Atmos. Sci.,* **40,** 1363–1392.

Wallace, J. M., and V. E. Kousky, 1968: Observational evidence of Kelvin waves in the tropical stratosphere. *J. Atmos. Sci.,* **25,** 900–907.

Webster, P. J., 1972: Response of the tropical atmosphere to local steady forcing. *Mon. Wea. Rev.,* **100,** 518–540.

——, 1973: Temporal variation of low latitude zonal circulations. *Mon. Wea. Rev.,* **101,** 803–816.

——, 1981: Mechanisms determining the atmospheric response to sea surface temperature anomalies. *J. Atmos. Sci.,* **38,** 554–571.

——, 1982: Seasonality in the local and remote response to sea surface temperature anomalies. *J. Atmos. Sci.,* **39,** 41–52.

——, 1983: Large-scale structure of the tropical atmosphere. *Large-scale Dynamical Processes in the Atmosphere,* B. J. Hoskins and R. P. Pearce, Eds., Academic Press, 392.

——, and J. R. Holton, 1982: Cross equatorial response to mid-latitude forcing in a zonally varying basic state. *J. Atmos. Sci.,* **39,** 722–733.

Weikman, K. M., G. R. Lussky and J. E. Kutzbach, 1985: Intraseasonal (30–60 day) fluctuations of outgoing longwave radiation and 250 mb stream function during northern winter. *Mon. Wea. Rev.,* **113,** 941–961.

Williams, M., 1981: Interhemispheric interaction during Winter MONEX. *Proceedings* International Conference on Early Results of FGGE and the Large-scale Aspects of its Monsoon Experiments, 10, 12–16, World Meteor. Organization.

Whitham, G. B., 1965: A general approach to linear and non-linear dispersive waves using a Lagrangian. *J. Fluid Mech.,* **22,** 273–283.

Yanai, M., and T. Mauryama, 1966: Stratospheric wave disturbance propagating over the equatorial Pacific. *J. Meteor. Soc. Japan,* **44,** 291–294.